Molecular Neurobiology (2019) 56:1167–1187
https://doi.org/10.1007/s12035-018-1135-4

The Mycobacterial Adjuvant Analogue TDB Attenuates Neuroinflammation via Mincle-Independent PLC-γ1/PKC/ERK Signaling and Microglial Polarization

Mahendravarman Mohanraj[1] · Ponarulselvam Sekar[1] · Horng-Huei Liou[2,3] · Shwu-Fen Chang[1] · Wan-Wan Lin[1,2]

Received: 3 November 2017 / Accepted: 18 May 2018 / Published online: 6 June 2018

Abstract

Microglial activation has long been recognized as a hallmark of neuroinflammation. Recently, the bacillus Calmette-Guerin (BCG) vaccine has been reported to exert neuroprotective effects against several neurodegenerative disorders. Trehalose-6,6′-dibehenate (TDB) is a synthetic analogue of trehalose-6,6′-dimycolate (TDM, also known as the mycobacterial cord factor) and is a new adjuvant of tuberculosis subunit vaccine currently in clinical trials. Both TDM and TDB can activate macrophages and dendritic cells through binding to C-type lectin receptor Mincle; however, its action mechanism in microglia and their relationship with neuroinflammation are still unknown. In this article, we found that TDB inhibited LPS-induced M1 microglial polarization in primary microglia and BV-2 cells. However, TDB itself had no effects on IKK, p38, and JNK activities or cytokine expression. In contrast, TDB activated ERK1/2 through PLC-γ1/PKC signaling and in turn decreased LPS-induced NF-κB nuclear translocation. Furthermore, TDB-induced AMPK activation via PLC-γ1/calcium/CaMKKβ-dependent pathway and thereby enhanced M2 gene expressions. Interestingly, knocking out Mincle did not alter the anti-inflammatory and M2 polarization effects of TDB in microglia. Conditional media from LPS-stimulated microglial cells can induce in vitro neurotoxicity, and this action was attenuated by TDB. Using a mouse neuroinflammation model, we found that TDB suppressed LPS-induced M1 microglial activation and sickness behavior, but promoted M2 microglial polarization in both WT and Mincle$^{-/-}$ mice. Taken together, our results suggest that TDB can act independently of Mincle to inhibit LPS-induced inflammatory response through PLC-γ1/PKC/ERK signaling and promote microglial polarization towards M2 phenotype via PLC-γ1/calcium/CaMKKβ/AMPK pathway. Thus, TDB may be a promising therapeutic agent for the treatment of neuroinflammatory diseases.

Keywords TDB · Neuroinflammation · Mincle · AMPK · Microglial polarization

Introduction

Microglia, the resident macrophages of the central nervous system (CNS), are inactive under physiological conditions and become activated in case of brain injury resulting from trauma or infection [1]. The activated microglial cells can migrate towards the site of injury and induce productions of nitric oxide, reactive oxygen species, pro-inflammatory cytokines, and chemokines [2, 3]. These secreted factors are essential for the polarization of microglia into what has been termed a classical phenotype (M1) and alternative phenotype (M2) [4]. Activation of the M1 phenotype favors the production and release of cytokines that exacerbate neural injury. In contrast, activation of the M2 phenotype triggers the release of neurotrophic factors that promote CNS repair [5]. Alterations in microglial M1/M2 phenotype have also been implicated in various neurodegenerative diseases such as multiple sclerosis, Alzheimer's disease, and Parkinson's disease [4, 6]. Thus, switching microglia from M1 to M2 phenotype may be a promising therapeutic approach to treat inflammation-associated disorders [5].

Electronic supplementary material The online version of this article (https://doi.org/10.1007/s12035-018-1135-4) contains supplementary material, which is available to authorized users.

✉ Wan-Wan Lin
wwllaura1119@ntu.edu.tw

[1] Graduate Institute of Medical Sciences, Taipei Medical University, Taipei, Taiwan

[2] Department of Pharmacology, College of Medicine, National Taiwan University, Taipei, Taiwan

[3] Department of Neurology, National Taiwan University, Taipei, Taiwan

Mycobacterium bovis bacillus Calmette-Guérin (BCG) is the only licensed vaccine that is commonly used against tuberculosis (TB) worldwide [7]. However, BCG vaccination is moderately effective against the progression of infection to disseminated TB and tuberculosis meningitis (TBM) in infants and young children [8]. Recent studies have demonstrated that BCG vaccine can induce a neuroprotective immune response under several neuropathological conditions. Early BCG may benefit clinically syndrome in patients with multiple sclerosis and its long-term course [9]. In mouse models of Parkinson's disease [10] and cognitive deficit Alzheimer's disease [11], BCG alleviates neuroinflammation and induces neuroprotection. Moreover, mycobacterial BCG injection in the CNS suppresses experimental autoimmune encephalomyelitis and Th17 responses in an IFN-γ-independent manner [12]. Similarly, the neonatal BCG vaccination improves neurogenesis and mouse sickness behavior in early life by inducing M2 microglial activation [13, 14]. Upon neonatal BCG vaccination, there is evidence of alleviation of neurobehavioral impairments and neuroinflammation induced by LPS challenge in adult mice [15]. However, to date, the potential components of BCG and their neuroprotective mechanisms are still unclear.

Among mycobacterial components, trehalose-6,6′-dimycolate (TDM, also known as cord factor) is the most abundant glycolipid found in the cell wall of *Mycobacterium tuberculosis* (*Mtb*) and other *Mycobacteria* species [16, 17]. TDM possesses immunostimulatory properties, including granuloma genesis and adjuvant activity for cell-mediated and humoral immune responses [18]. Its synthetic analogue trehalose-6,6′-dibehenate (TDB) is a new adjuvant currently in phase I clinical trial for tuberculosis subunit vaccine [19, 20]. In rodents, both TDM and TDB have the affinity for binding to C-type lectin Mincle receptors to activate macrophages and dendritic cells [21, 22]. Upon TDB recognition, Mincle interacts with immune receptor FcRγ, thus activating spleen tyrosine kinase (Syk), which in turn induces CARD9/BCL10/MALT1 complex and nuclear factor kappa B (NF- B) activation. Furthermore, Syk can induce intracellular calcium mobilization and the subsequent calcineurin-NFAT activation [22, 23]. In the brain, Mincle-Syk signal cascade was reported to play crucial roles in the pathogenesis of ischemic stroke [24] and the promotion of excessive innate immune response following subarachnoid hemorrhage [25]. In a trauma murine model and clinical subjects, a drastic increase in the Mincle expression was found in cerebrospinal fluid and brain tissue, suggesting the involvement of Mincle in traumatic brain injury pathology [26, 27]. Nevertheless, Mincle was also reported to have dual functions in the promotion and subsequent resolution of inflammation [28]. In addition, a recent study revealed that Mincle mediates TDB-induced suppression of TLR4-induced response in mouse splenocytes and macrophages by upregulation of p38-dependent inhibitory intermediates SOCS1, A20, and ABIN3 [29]. Thus, the actual role of Mincle in neuroinflammation remains poorly understood and might be context dependent.

To date, most efforts to understand signaling pathways elicited by TDB have been studied mainly in peripheral immune cells, and very little is known about the TDB-specific responses in the brain and its action mechanisms in microglia. Therefore, the aim of this study is to investigate the effects of TDB on microglial polarization in both in vitro and in vivo models of neuroinflammation.

Materials and Methods

Animals

WT (C57BL/6) mice were purchased from Laboratory Animal Center, National Taiwan University. The Mincle$^{-/-}$ mice were a generous gift from Dr. Shie-Liang Hsieh (Genomics Research Center, Academia Sinica, Taipei, Taiwan). All animals were bred under specific pathogen-free conditions in the Laboratory Animal Center, National Taiwan University College of Medicine (Taipei, Taiwan). All experimental procedures were approved by the National Taiwan University College of Medicine Ethics Committee in accordance with their guidelines for the care of animals (protocol no. 20110047).

Reagents

TDB was from InvivoGen (San Diego, CA, USA). Lipopolysaccharide (LPS), MTT, protease inhibitor cocktails, ionomycin, BAPTA-AM, U-73122, and STO-609 were from Sigma-Aldrich (St. Louis, MO, USA). U0126, GF109203X, and A769662 were from Calbiochem (San Diego, CA, USA). The Syk inhibitor R406 was from Selleck Chemicals LLC (Houston, TX, USA). Antibodies directed against Syk (1:1000; sc-1077), PLC-γ1 (1:1000; sc-81), p38 (1:1000; sc-81621), JNK1 (1:1000; sc-1648), ERK2 (1:1000; sc-1647), IKKα (1:500; sc-7182), IκBα (1:1000; sc-371), p65 (1:1000; sc-8008), p50 (1:1000; sc-7178), CaMKK2 (1:1000; sc - 50341) arginase-1 (1:500; sc-20150), COX-2 (1:500; sc-1745), IL-6 (1:500; sc-57315), and HRP-coupled anti-rabbit and anti-mouse secondary antibodies were from Santa Cruz Biotechnology (Santa Cruz, CA, USA). Anti-inducible NO synthase (iNOS) (1:500; cat. no. 610329) polyclonal antibody was from BD Biosciences (Franklin Lakes, NJ, USA). Mincle antibody (1:500; code no. 292-3) was from MBL (Woburn, MA, USA). Iba-1 antibody (1:500; cat. no. 016-20001) was from WAKO (Wako Chemicals USA, Inc., Richmond, VA, USA). Anti-FcRγ subunit (1:500; cat. no. 06-727) was from Millipore (Temecula, CA, USA). Mouse anti-Mincle neutralizing antibody (cat. code mabg-mmcl) and its isotype control IgG antibody (cat. code mabg2b-ctlrt) were

from InvivoGen (San Diego, CA, USA). Specific antibodies against AMPKα (1:1000; #2532), Acetyl-CoA carboxylase (ACC) (1:1000; #3662), AKT (1:1000; #9272), LKB1 (1:1000; #3050), and phosphorylated forms of Syk (Tyr525/526) (1:1000; #2711), PLC-1γ (Tyr783) (1:1000; #2821), PKC (1:1000; #9371), p38 MAPK (Thr180/Tyr182) (1:1000; #9211), JNK (Thr183/Tyr185) (1:1000; #9251), ERK (Thr202/Tyr204) (1:1000; #9106), IKKα/β (Ser176/Ser180) (1:1000; #2697), AMPKα (T172) (1:1000; #2535), ACC (Ser59) (1:1000; #3661), CaMKK2 (Ser511) (1:1000; #12818), and LKB1 (Ser428) (1:1000; #3482) were from Cell Signaling Technology (Danvers, MA, USA). Antibody against β-actin (1:1000; MAB1501) was from Chemicon (International, Temecula, CA). Protein concentration was determined by a Bio-Rad protein assay kit (Bio-Rad, Richmond, CA, USA). Fluo-3AM was from Molecular Probes (Eugene, OR, USA). DMEM, trypsin-EDTA, and antibiotic penicillin/streptomycin were from Invitrogen (Rockville, MD, USA). TriPure isolation reagent was purchased from Roche Diagnostics (Indianapolis, IN, USA). Fluorescein isothiocyanate (FITC)-conjugated goat anti-rat IgG secondary antibody and Annexin V-FITC and propidium iodide (PI) were from Biolegend (San Diego, CA, USA). The ECL reagent Western Lightning Chemiluminescence Reagent Plus was from PerkinElmer (Wellesley, MA, USA). The FastStart SYBR Green Master was from Roche Applied Science (Nutley, NJ, USA).

Cell Culture

The immortalized murine microglial cell line, BV-2 has been widely used as an in vitro model to study neuroinflammation [29, 30]. BV-2 cells and SH-SY5Y human neuroblastoma cells were cultured in DMEM (Gibco, Grand Island, NY, USA) supplemented with 10% FBS, 100 U/ml penicillin, and 100 μg/ml streptomycin, and incubated at 37 °C in a humidified atmosphere containing 5% CO_2 and 95% air. Primary microglial culture was obtained by mild trypsinization method as described previously with slight modification [31]. After 14–21 days, the mixed glial cells from both WT and Mincle$^{-/-}$ mice were incubated with a trypsin solution (0.25% trypsin, 1 mM EDTA in Hank's balanced salt solution) diluted 1:4 in PBS containing 1 mM $CaCl_2$ for 30–60 min at 37 °C. This resulted in the detachment of the upper layer of astrocytes in one piece, while the microglia remained attached to the bottom of the culture flask. The detached layer of astrocytes was removed, and the remaining microglia were used for experiments. The purity of microglial cultures was assessed using CD11b antibody, and more than 95% of the cells were positive for CD11b. Primary cultures of dissociated cortical neurons were prepared from E17–20 mice according to previously described method [32]. Briefly, mouse embryos were decapitated, and the brains were immediately removed and placed in a petri dish containing ice-cold PBS. Cortices were harvested, then transferred to a culture dish containing 0.25% trypsin-EDTA for 30 min at 37 °C, and washed twice in a serum-free neurobasal medium. The cortical tissue was then mechanically dissociated by gentle pipetting and the resulting dissociated cortical cells were seeded onto plates pre-coated with poly-D-lysine in a neurobasal medium containing 2 mM glutamine, penicillin–streptomycin, nerve growth factor, N-2 supplement, and B-27 supplement.

MTT Assay

Mouse BV-2 microglial cells (1×10^4/ml) were plated in 96-well plates. After 24 h of incubation, cells were then treated with the indicated agents or vehicle at 37 °C for 24 h. MTT (5 mg/ml) was added for 1 h and then the culture medium was aspirated. The formazan granules generated by live cells were dissolved in DMSO with gentle shaking for 10 min. The OD values at 550 and 630 nm were measured using a microplate reader. The net absorbance (OD550–OD630) indicated the enzymatic activity of mitochondria and implicated in cell viability.

Nitrite Oxide Assay

Accumulation of nitrites in the culture medium was determined by a colorimetric assay with Griess reagent as previously described [30]. Murine BV-2 microglial cells were treated with TDB (or vehicle) and/or LPS at the indicated concentrations for 16 h. Aliquots of conditioned media were mixed with an equal volume of Griess reagent (1% sulphanilamide and 0.1% N-(1-naphthyl)-ethylenediamine in 5% phosphoric acid). Nitrite concentrations were determined by comparison with the OD550 using standard solutions of sodium nitrite prepared in the culture medium.

Subcellular Fractionation and Immunoblot Analysis

After the indicated treatment, the medium was aspirated. The nuclear and cytoplasmic extracts were prepared by hypotonic or Nonidet P-40 detergent lysis buffer as previously described [33]. Briefly, cells were washed with ice-cold PBS and then lysed in hypotonic buffer (10 mM HEPES pH 7.9, 10 mM KCl, 1.5 mM $MgCl_2$, 0.34 M sucrose, 10% glycerol, 0.1% Triton X-100, 1 mM DTT, 0.1 mM PMSF) supplemented with proteinase inhibitors (Calbiochem) for 5 min on ice. The lysates were spun down at 1300 rpm, 4 °C for 15 min. The supernatant (cytoplasmic extract) was further cleared by centrifugation at 13,000 rpm at 4 °C for 15 min. The pelleted nuclei were washed with hypotonic buffer and then resuspended in nuclear lysis buffer (20 mM HEPES pH 7.9, 300 mM KCl,

0.01% Triton X-100, 0.5 mM EDTA, 0.1 mM PMSF, 1 mM DTT) containing proteinase inhibitors. Nuclei were then homogenized on ice for 30 min using a dounce homogenizer for 20 strokes. The supernatant (nuclear extract) was collected by centrifugation at 16,000 rpm for 15 min. Both cytoplasmic and nuclear extracts were dialyzed against D100 buffer (20 mM HEPES pH 7.9, 100 mM KCl, 0.2 mM PMSF). For whole lysates, cells were harvested and lysed in radioimmunoprecipitation assay (RIPA) lysis buffer (50 mM Tris-HCl pH 7.6, 150 mM NaCl, 1% Triton X-100, 0.1% SDS, 0.1% deoxycholate, 2 mM EDTA, 2 mM NaF, 2 mM Na_3VO_4, 1 mM PMSF, and protease inhibitor cocktails) followed by centrifugation at 12,500 rpm, 4 °C for 15 min. The protein concentrations were measured by a Bio-Rad protein assay reagent. Protein expression was determined in cell lysates by SDS-PAGE followed by immunoblotting as we have previously described [34].

Quantitative Real-time PCR

Murine mRNA expressions of iNOS, COX-2, TNF-α, IL-1β, IL-6, IL-10, Mincle, IFN-β, MIP2, and β-actin (Supplementary Table 1) were determined by real-time PCR analysis. After drug or vehicle treatment, cells were homogenized with 200 μl of TriPure isolation reagents (Roche Applied Science), and 1 μg of total RNA was reverse-transcribed with an RT-PCR kit (Promega) according to the manufacturer's instructions. Real-time PCR was performed in 96-well plates with the Fast Start SYBR Green Master. Each 25-μl PCR well contained complementary DNA (cDNA), Master Mix, gene-specific primers, and passive reference dye (ROX) to normalize the signals from the SYBR Green-double-stranded DNA complexes during the analysis and to correct for well-to-well variations. PCR products were measured with an ABI Prism 7900 (Applied Biosystems, Foster City, CA, USA).

RNA Interference

Mouse si-AMPKα1/2 (cat. no. SC-45313) and scramble non-specific siRNA were purchased from Santa Cruz Biotechnology (Santa Cruz, CA, USA). BV-2 microglial cells were transfected with 100 nM siRNA by DharmaFECT transfection reagents (Dharmacon Research, Lafayette, CO, USA) at 50% confluence following the manufacturer's instruction. After siRNA transfection for 48 h, cells were harvested after treatment with the indicated drugs.

Flow Cytometry Analysis

After treatment for the indicated time periods, cells were collected and washed with PBS twice, then incubated in PBS containing 25 μg/ml Annexin V/PI staining (for the detection of cell death) or 3 μM Fluo-3AM (for the detection of intracellular calcium mobilization) for 30 min at 37 °C. To examine surface expression of Mincle after drug or vehicle treatment, cells were incubated with anti-Mincle antibody for 60 min at 4 °C followed by washing and incubation with FITC-conjugated goat anti-rat IgG for 45 min at 4 °C. After incubation cells were washed and resuspended in PBS with 1% BSA. The fluorescence intensity was measured by flow cytometry (BD FACSCalibur Franklin Lakes, NJ, USA) and the data were analyzed using Cell Quest software.

Microglia-Derived Conditioned Media

To obtain microglia-derived conditioned media (MCM), BV-2 cells and WT and Mincle$^{-/-}$ primary microglia were stimulated with TDB (50 μg/ml), vehicle, and/or LPS (0.1 μg/ml) for 5 h. The cells were then washed with PBS and cultured in fresh DMEM medium for an additional 24 h. Conditioned media were collected and centrifuged to remove cellular debris. MCM were added to SH-SY5Y cells or primary neurons derived from WT mice and then incubated for 24 h. Neuronal viability was then assessed using the MTT assay as described above.

Immunoprecipitation

After the indicated drug treatment, cells were harvested and co-immunoprecipitated with specific antibody followed by immunoblotting analysis as described previously [33].

Seahorse Analysis of Mitochondrial Bioenergetics

The oxygen consumption rate (OCR) and extracellular acidification rate (ECAR) were measured using the XF-24 Analyzer (Seahorse Bioscience, Houston, TX, USA) as previously described [35, 36]. BV-2 cells were seeded onto XF-24 cell culture microplates and transfected with si-AMPK or si-Ctrl as described above, and 48 h later, cells were treated with indicated drugs for 16 h. The medium was then removed, and cells were washed with 1 ml of XF running media, followed by the addition of 750 μl of XF running media. Prior to the start of an experiment, cells were incubated for 1 h at 37 °C in an incubator without CO_2. On the day before the experiment, 1 ml of XF calibration medium was added to the XF sensor cartridges and kept in a non-CO_2 incubator overnight. On the day of the experiment, XF sensor cartridges were then placed onto XF-24 instrument and calibrated. At the time of measurement, sample plates were inserted into the XF24 Flux Analyzer with cartridges of probes. OCR was measured at every 8-min time point before and after the injection of the following compounds: (i) oligomycin (2.5 μM), (ii) FCCP

(1 μM), and (iii) antimycin (2.5 μM) + rotenone (2.5 μM). The glycolysis stress assay indexed by ECAR was performed in a similar manner, with subsequent injection of the following compounds: glucose (5.0 mM), oligomycin (2.5 μM), and 2-deoxy-D-glucose (2-DG) (7.5 mM). OCR and ECAR data were then analyzed and plotted by Seahorse XF24 software (version 1.8).

Neuroinflammation and Behavioral Studies in Mice

Male, 4- to 8-week-old WT and Mincle$^{-/-}$ mice were randomized into four groups (five animals per group): vehicle control, TDB, LPS, and TDB + LPS groups. LPS was dissolved in saline, and TDB solution was prepared by mixing 1.0 ml of PBS with 2 μl DMSO (0.2% final) to a vial containing 1.0 mg of TDB. The TDB suspension was sonicated to ensure complete solubilization. The vehicle control group was intraperitoneally administered with a single dose of saline containing 0.01% DMSO daily for 1 week. The TDB group was intraperitoneally injected with TDB (50 μg/mouse) every alternate day in a week as previously described [37, 38]. The LPS group was intraperitoneally given a single dose of LPS (330 μg/kg) daily for 1 week. The dosage of LPS was chosen based on the previous study of LPS-induced murine neuroinflammation model [29, 39]. The co-treatment group (TDB + LPS) was intraperitoneally administered with TDB (50 μg/mouse) on days 2, 4, and 6 along with 330 μg/kg LPS daily for 1 week. Animals were monitored daily for body weight and food intake during the course of the experiment. Open-field test was performed 8 h after the final LPS challenge to evaluate behavioral activity as previously described [39]. WT and Mincle$^{-/-}$ mice were placed in the center of an open arena (48 × 48 × 40 cm^3); the number of line crossings (forelimbs crossing a line) and rearings (standing on hind legs, without contact with the sides of the arena) were counted over a 5-min period and the data were recorded. After behavioral assessment, the animals were sacrificed; whole brains were harvested and dissected into hippocampus and cerebellum regions. Brain tissues were stored at − 80 °C until further analysis. Briefly, the brain tissues were homogenized in RIPA lysis buffer on ice and supernatants were collected and subjected to Western blot analysis.

Statistical Analysis

Values were expressed as mean ± SEM (standard error mean) of at least three independent experiments. Student's *t* tests were used to assess the statistical significance of differences between the experimental and the vehicle control groups. A value of $p < 0.05$ was considered statistically significant.

Results

TDB Suppresses LPS-Induced Inflammatory Responses in BV-2 Microglial Cells

To assess the role of TDB in LPS-induced inflammatory responses, we first determined the effects of TDB and LPS, either alone or in combination, in murine BV-2 microglial cells. We found that TDB (10–50 μg/ml) treatment alone for 16 h had no effects on nitrite oxide (NO) production and iNOS and proIL-1β protein expression (Fig. 1a, b). In addition, there was no significant effect on inflammatory gene expression in BV-2 cells after incubation with TDB (50 μg/ml) for 2 and 5 h (Fig. 1d). Increasing TDB treatment for up to 48 h still cannot change gene levels of COX-2, iNOS, TNF-α, proIL-1β, IL-6, IFN-β, MIP2, and Mincle (data not shown). Interestingly, combination of TDB (20 and 50 μg/ml) with LPS (100 ng/ml) significantly reduced NO production (Fig. 1a). Moreover, LPS-induced iNOS and proIL-1β protein expressions were significantly decreased upon co-treatment with TDB in concentration- and time-dependent manners. In contrast, LPS-induced COX-2 protein expression was unaffected by TDB (Fig. 1c). Subsequently, we sought to determine whether TDB inhibits the LPS-induced production of inflammatory cytokines at the transcriptional level in BV-2 microglia. As expected, stimulation of BV-2 cells with LPS (100 ng/ml) for 2 and 5 h dramatically increased gene expressions of iNOS, COX-2, TNF-α, proIL-1β, IL-6, IFN-β, and MIP2, and these gene expressions except COX-2 were inhibited by TDB (Fig. 1d). In order to exclude the possibility that the anti-inflammatory effects of TDB were due to cytotoxicity, cell viability was assessed. BV-2 microglial cells were incubated at various concentrations of TDB (10, 20, and 50 μg/ml) and LPS (100 ng/ml) alone or in combination. Following 24-h treatment, we found that only TDB at 20 or 50 μg/ml caused a slight decrease (5–10%) in cell viability when analyzed by Annexin V/PI staining (Fig. 1e, f) and MTT assay (Fig. 1g). Because no cell death was observed after 16-h treatment (data not shown), the inhibition of LPS response by TDB observed at 2–5 h is not a consequence of general cytotoxicity. Instead, a specific pathway associated with TDB might be involved in modulation of inflammatory responses in microglial cells.

TDB and LPS Synergistically Activate ERK via PLC-γ1-PKC-Dependent Pathway but Independent of Syk

To understand the molecular mechanisms for TDB-induced inhibition of pro-inflammatory responses in LPS-stimulated BV-2 cells, we examined the signaling cascades triggered by TDB and LPS. Firstly, we found that TDB alone can activate Syk, p38, and ERK1/2 with mild activation of JNK at 30 min. Moreover, p38 and ERK1/2, but not Syk and JNK, sustained

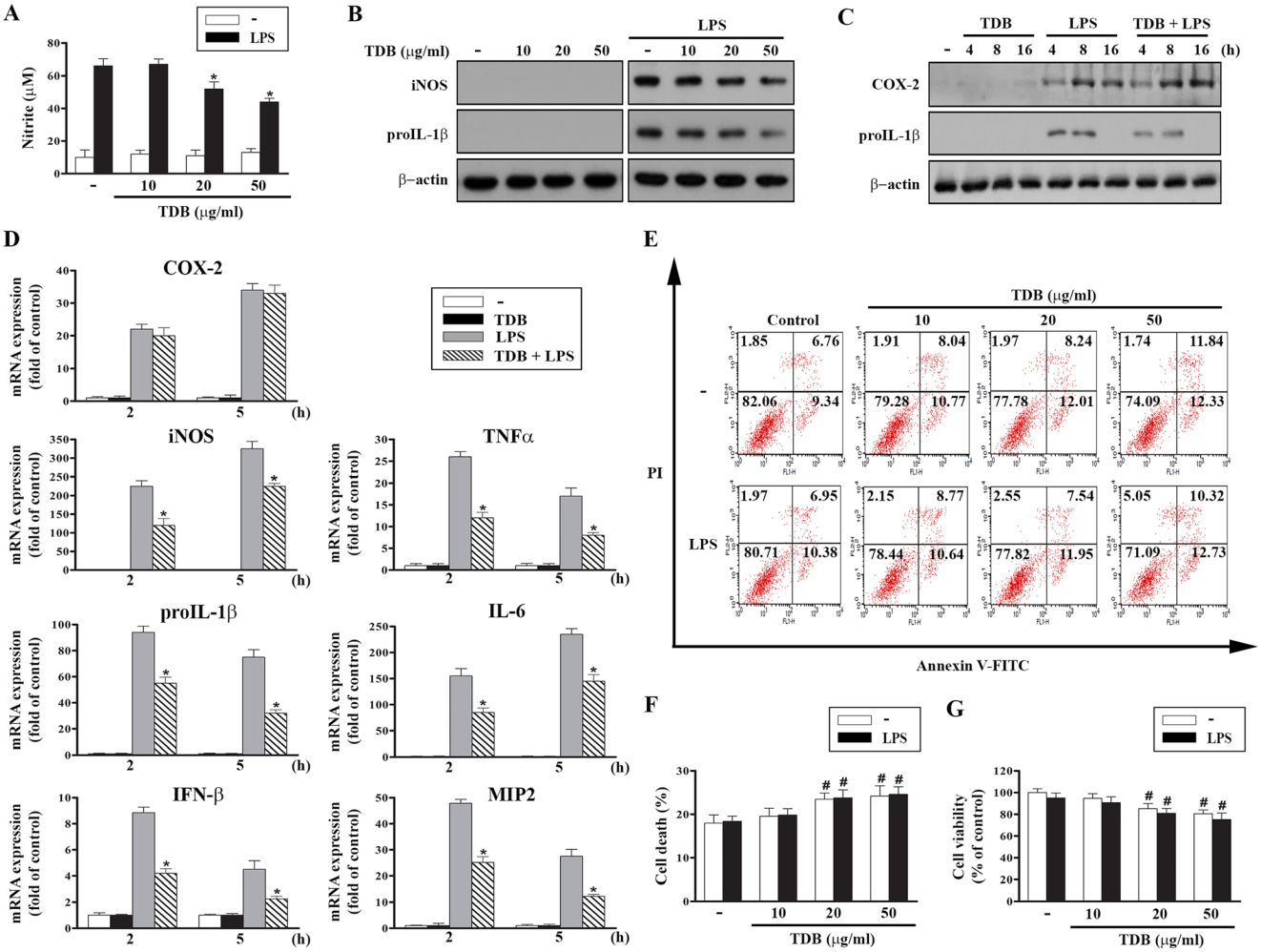

Fig. 1 *TDB inhibits LPS-induced inflammatory gene expression in BV-2 microglial cells*. Cells were treated with vehicle (0.01% DMSO) or co-treated with TDB (10–50 μg/ml) and/or LPS (100 ng/ml) at different intervals as indicated. **a** After drug treatment for 16 h, the nitrite production in the supernatants was measured. **b** Total cell lysates prepared at 8 h (for proIL-1β) or 16 h (for iNOS) were subjected to SDS-PAGE followed by immunoblotting analysis. **c** After treatment with vehicle (0.01% DMSO) or TDB (50 μg/ml) and/or LPS for different periods, COX-2 and proIL-1β were determined by immunoblotting. β-actin was detected as a loading control. **d** After incubation for different intervals with TDB (50 μg/ml) and/or LPS, total mRNA was extracted and reversely transcribed for quantitative PCR analyses of iNOS, COX-2, TNF-α, proIL-1β, IL-6, IFN-β, and MIP2 gene expression. Values were normalized to β-actin gene expression and expressed relative to the vehicle control group. **e**–**g** Cells were treated with vehicle (0.01% DMSO) or co-treated with TDB and/or LPS for 24 h; cell viability was assessed by propidium iodide (PI) and FITC-labeled Annexin V staining (**e**, **f**) and by MTT assay (**g**). Data were presented as mean ± SEM from at least three independent experiments. $^{*}p < 0.05$, indicating significant inhibition of LPS-induced responses by TDB; $^{\#}p < 0.05$, indicating a slight but significant effect of TDB on cell viability

their activation up to 1 h (Fig. 2a, c). Further, we examined the effect of TDB on NF-κB activation and found that TDB alone did not induce IKKα/β phosphorylation (Fig. 2a, c). In contrast, LPS induced IκBα degradation and stronger phosphorylation of p38, JNK, and IKKα/β than ERK1/2. However, Syk phosphorylation was detected after 15 min of LPS stimulation and declined to near basal levels by 30 min (Fig. 2a, b). Irrespective of the TDB co-treatment with LPS (Fig. 2a, c) or 30-min pre-treatment before LPS (Fig. 2b), an enhanced phosphorylation of ERK1/2 was observed as compared with TDB or LPS alone. Nevertheless, trivial changes were observed in the phosphorylation levels of Syk, p38, JNK, and IKKα/β upon co-treatment with TDB and LPS (Fig. 2a, c). Furthermore, no significant effects were found in FcRγ protein expression (Fig. 2a, b). We also determined another common adaptor of CLRs, DAP12, and it turned out undetectable in BV-2 cells (data not shown).

Previous studies demonstrated that Syk activation plays an important role in regulating TLRs signaling in immune cells including macrophages [33], dendritic cells [40], and neutrophils [41]. Therefore, we used R406, the specific inhibitor of Syk, to examine whether Syk is involved in TDB-induced ERK activation. Cells were pre-incubated with R406 for 30 min and then stimulated with TDB and LPS alone or in combination for the indicated time intervals. We found that R406 did not affect TDB-induced phosphorylation of p38,

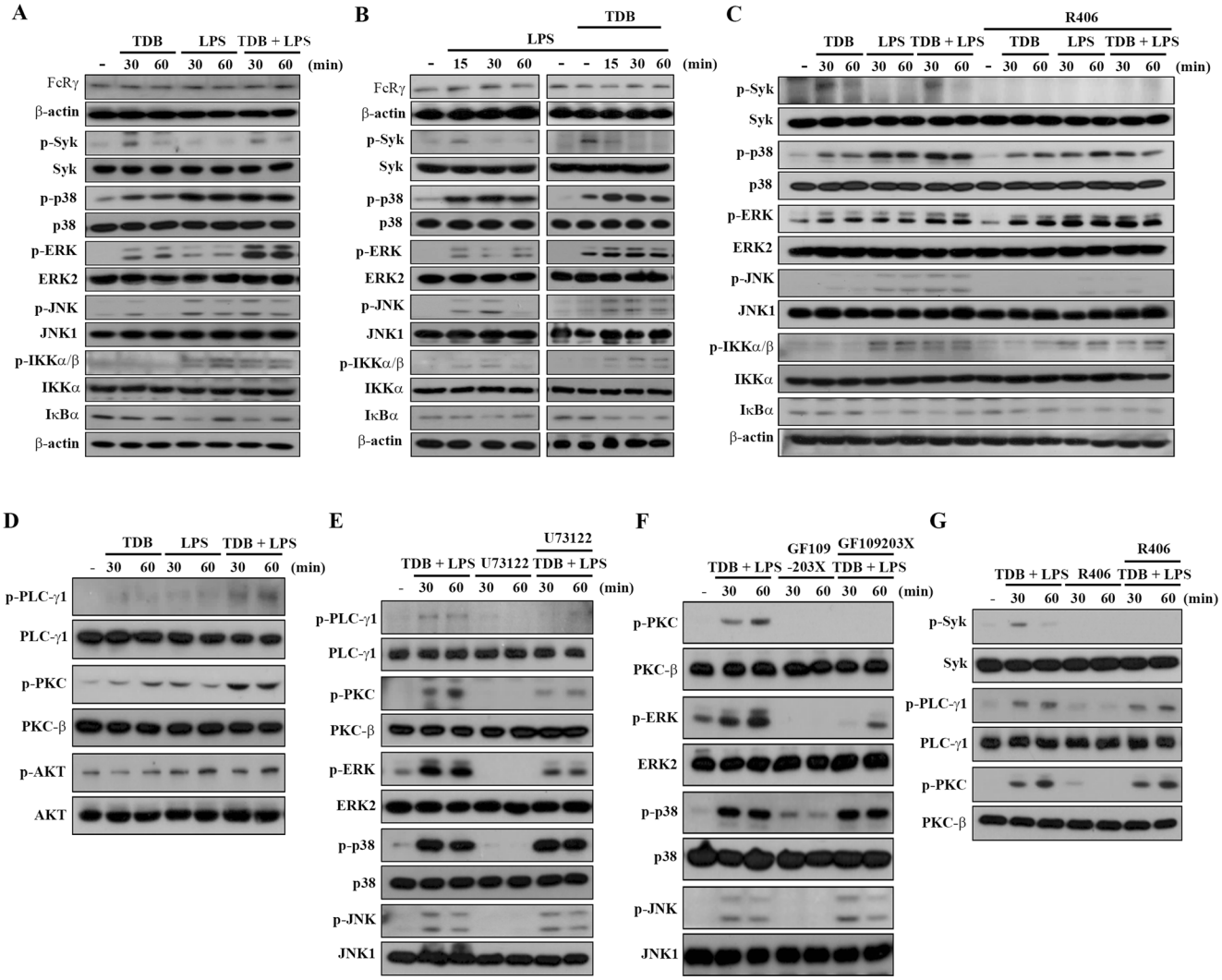

Fig. 2 *Synergistic phosphorylation of ERK by TDB and LPS through PLC-γ1-PKC pathway but independent of Syk.* **a** BV-2 microglial cells were treated with vehicle or co-treated with TDB (50 μg/ml) and/or LPS (100 ng/ml) for different time periods as indicated except in **b**. Cells were treated with vehicle or pre-treated with TDB for 30 min followed by LPS. In some experiments, cells were treated with vehicle or pre-treated with R406 (1 μM, Syk inhibitor) (**c**, **g**), U73122 (5 μM, PLC-γ inhibitor) (**e**), or GF109203X (5 μM, non-selective PKC inhibitor) (**f**) for 30 min before TDB and/or LPS stimulation. Total cell lysates were subjected to SDS-PAGE followed by immunoblotting analysis. Results were representative from three independent experiments

ERK, or JNK. Nevertheless, R406 decreased LPS-induced p38 and JNK, while increased the phosphorylation of ERK1/2 (Fig. 2c). On the contrary, R406 did not affect IKKα/β phosphorylation or IκBα degradation in cells treated with LPS. These results demonstrate that TDB and LPS induce different signaling cascades in BV-2 cells, i.e., the prominent and independent manner of Syk and ERK activation by TDB, and the stronger IKK, p38, and JNK activation in response to LPS.

Next, we determined the upstream signaling responsible for ERK activation during TDB and LPS treatments in BV-2 cells. As shown in Fig. 2d, TDB alone moderately increased PLC-γ1 and PKC, but not AKT phosphorylation. As anticipated, LPS stimulation of BV-2 cells induced phosphorylation of PKC and AKT, whereas it had only a slight effect on PLC-γ1. Interestingly, co-treatment of TDB and LPS led to synergistic increases in PLC-γ1 and PKC phosphorylation, while AKT phosphorylation caused by LPS was unchanged after TDB co-treatment. Furthermore, pre-treatment of cells with PLC inhibitor (U73122) or PKC inhibitor (GF109203X) attenuated TDB-induced ERK phosphorylation in LPS-activated BV-2 cells. Moreover, both inhibitors did not affect p38 and JNK phosphorylation upon co-treatment with TDB and LPS (Fig. 2e, f), suggesting that ERK activation by TDB plus LPS is via PLC-γ1-PKC signaling pathway. Because Syk has been reported to mediate Mincle-associated PLC-γ phosphorylation in mast cells [42] as well as PKC activation for innate immunity [22], we further tested this possibility in BV-2 cells. As a result, R406 did not inhibit TDB-induced phosphorylation of PLC-γ1 and PKC

(Fig. 2g). Altogether, these results indicate that TDB-induced activation of ERK in LPS-stimulated BV-2 cells occurs through the Syk-independent but PLC-γ1/PKC-dependent pathway.

TDB Induces AMPK Activation via PLC-γ1/Ca^{2+}/CaMKKβ Signaling and Independent of Syk or PLC-γ1/PKC/ERK

Because AMPK has been demonstrated as a multifunctional anti-inflammatory protein [43] and can be activated via Ca^{2+}/CaMKKβ pathway [44], we further examined the role of AMPK in the anti-inflammatory action of TDB. First, we measured intracellular Ca^{2+} level and found the synergistic effect of TDB and LPS in this event (Fig. 3a). In addition to increase intracellular Ca^{2+} level, TDB and LPS co-treatment induced CaMKKβ and AMPK activation and subsequent ACC phosphorylation, but did not alter LKB phosphorylation (Fig. 3b). Confirming these changes resulting from Ca^{2+} signal, our data revealed the abilities of BAPTA/AM and ionomycin to block and mimic these effects of TDB plus LPS, respectively (Fig. 3c). Furthermore, CaMKK inhibitor STO-609 abolished AMPK activation and its downstream ACC phosphorylation (Fig. 3d). Similarly, PLC inhibitor U73122 exerted the inhibitory actions in CaMKKβ and AMPK/ACC (Fig. 3e), while R406 had no effects on these events (Fig. 3f). Taken together, these results suggest that the synergistic effect of TDB and LPS on PLC-γ1 activation is independent of Syk but mediates Ca^{2+}/CaMKKβ signaling pathway for AMPK activation.

Our results suggest that TDB can activate both PLC-γ1/PKC/ERK and PLC-γ1/CaMKKβ/AMPK pathways in LPS-treated BV-2 cells. To understand the potential signaling crosstalk, we next evaluated their association. Firstly, we

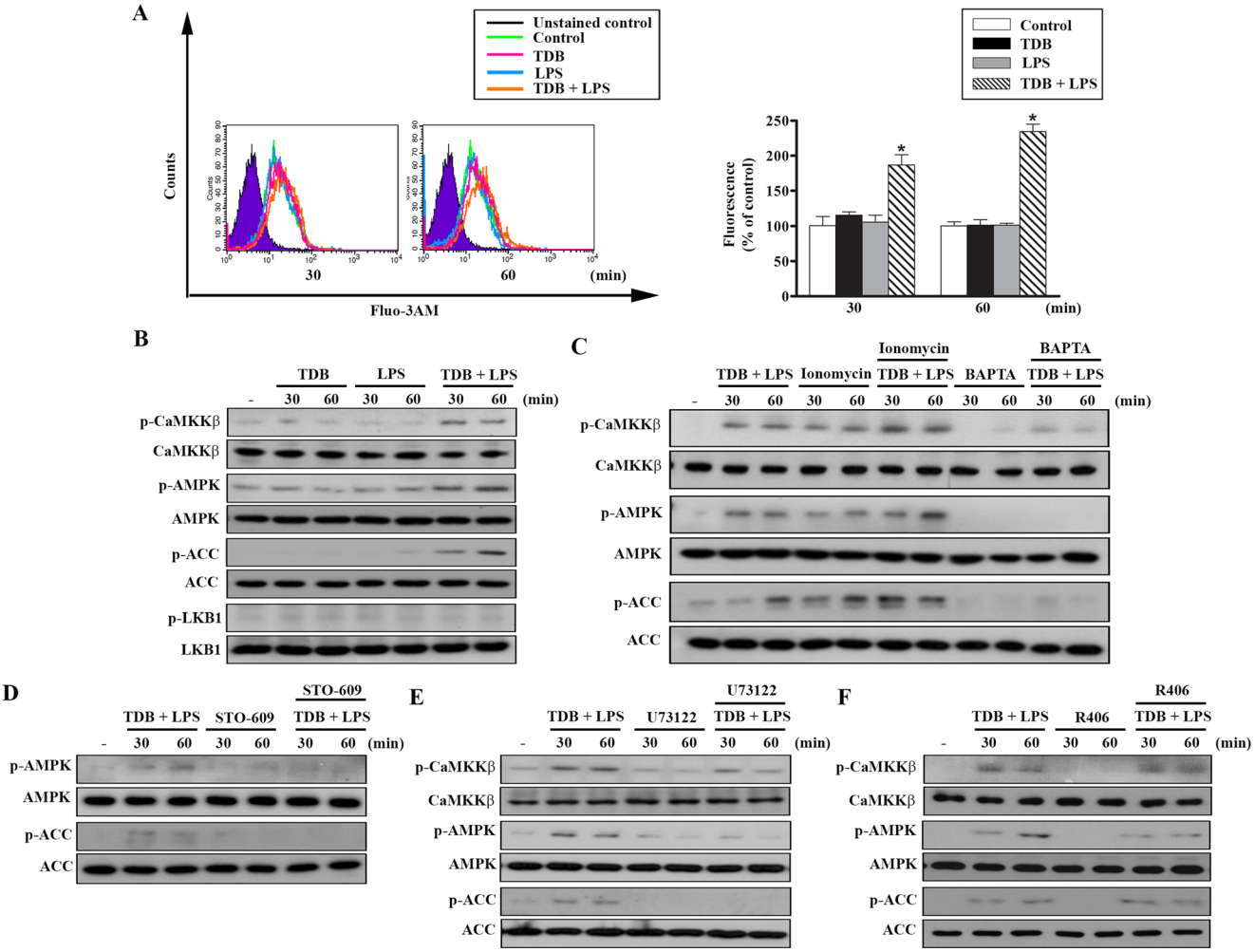

Fig. 3 *TDB-induced AMPK activation through PLC-γ1/Ca^{2+}/CaMKKβ signaling but independent of Syk*. **a** BV-2 cells were treated with vehicle or TDB (50 μg/ml) and/or LPS (100 ng/ml) for the indicated time periods. Intracellular calcium levels were determined by flow cytometry using Fluo-3AM. **b**–**f** After drug treatment, total cell lysates were subjected to SDS-PAGE followed by immunoblotting. In some experiments, cells were treated with vehicle or pre-treated with BAPTA/AM (2 μM) (**c**), STO-609 (10 μM) (**d**), U73122 (5 μM) (**e**), or R406 (1 μM) (**f**) for 30 min before TDB, LPS (100 ng/ml) (**c**–**f**), and/or ionomycin (5 μM) (**c**). Data were presented as mean ± SEM from three independent experiments. *$p < 0.05$, indicating a significant increase in intracellular calcium levels by TDB

examined whether the PKC/ERK pathway is involved in CaMKKβ/AMPK activation in TDB/LPS-stimulated BV-2 cells by using MEK inhibitor U0126 and PKC inhibitor GF109203X. The results showed that neither U0126 nor GF109203X inhibits TDB/LPS-induced phosphorylation of CaMKKβ, AMPK, ACC, p38, and/or JNK (Supplementary Fig. 1A, B). Secondly, we addressed the role of CaMKKβ/AMPK pathway in PKC and MAPK activation by using CaMKKβ inhibitor STO-609 and AMPK activator A769662. We found STO-609 failed to block PKC and MAPK activation (Supplementary Fig. 1C). While A769662 itself can induce AMPK and ACC phosphorylation, it cannot change MAPK activation caused by TDB/LPS (Supplementary Fig. 1D). Together, these results not only substantiate the diverse signaling cascades (PKC, ERK, CaMKKβ, and AMPK) in TDB/LPS-challenged BV-2 microglial cells but also demonstrate lack of crosstalk between PKC/ERK and CaMKKβ/AMPK signaling pathways.

ERK Activation Is Involved in the Anti-inflammatory Actions of TDB

After observing anti-inflammatory actions of TDB (Fig. 1d) and the synergistic activation of ERK by TDB and LPS (Fig. 2), we determined whether Syk and ERK activations contribute to the anti-inflammation outcome. As shown in Fig. 4a, pre-treatment with Syk inhibitor R406 significantly reduced LPS-induced expressions of pro-inflammatory markers (iNOS, TNF-α, proIL-1β, IL-6, IFN-β, and MIP2) when compared to LPS alone. Surprisingly, the addition of R406 resulted in an additive effect with TDB on the anti-inflammatory actions. In contrast, U0126 alone failed to affect the LPS-induced inflammatory gene expression in BV-2 cells, but entirely blocked the effects of TDB (Fig. 4a). These data revealed that TDB can exert its anti-inflammatory effect through ERK but not Syk signaling pathway.

We then investigated the molecular mechanism on ERK downstream signaling and the underlying anti-inflammatory action of TDB in BV-2 cells. Firstly, we examined whether TDB-induced activation of ERK affects the nuclear translocation of NF-κB in LPS-stimulated BV-2 cells. TDB (50 μg/ml) alone had no effect on NF-κB nuclear translocation. Predictably, LPS treatment increased the levels of NF-κB nuclear translocation at 30 min and 1 h. It is interesting to note that TDB treatment significantly decreased LPS-induced nuclear translocation of NF-κB/p65 but not NF-κB/p50, concomitantly by the accumulation of NF-κB/p65 in the cytosol (Fig. 4b). Pre-treatment of cells with the specific ERK inhibitor U0126 significantly reversed the inhibitory effect of TDB on NF-κB nuclear translocation (Fig. 4c). Co-immunoprecipitation data further revealed the association of ERK with p65, but not with p50, upon TDB and LPS co-stimulation (Fig. 4d) and this association can be observed in both cytosol and nuclei (Fig. 4e). Taken together, these results suggest that the TDB-induced ERK activation leads to the inhibition of LPS-induced nuclear translocation of NF-κB/p65, thereby providing a potential mechanism for TDB-induced downregulation of pro-inflammatory genes.

Differential Involvement of AMPK in TDB-Induced Anti-inflammation, M2 Polarization, and Metabolic States

Next, we determined whether AMPK activation is involved in TDB-induced anti-inflammatory effect in activated microglia by using siRNA approach. As shown in Fig. 5a, AMPK siRNA transfection significantly reduced AMPK expression compared with non-sense control siRNA (si-Ctrl) transfection. AMPKα knockdown augmented LPS-induced M1 marker genes (iNOS, TNF-α, proIL-1β, IL-6, IFN-β, and MIP2). However, AMPK silencing did not affect the suppressive activity of TDB on M1 inflammation (Fig. 5a). Previous studies showed that AMPK activation promotes M2 polarization of microglia [29], so we examined the influence of AMPK knockdown on TDB-elicited expression of M2-specific markers in LPS-stimulated BV-2 cells. Like macrophages, microglial polarization from classical pro-inflammatory M1 phenotype to alternative anti-inflammatory M2 phenotype represents a potential pharmacological target in neuroinflammatory diseases [35, 45]. Treatment with either TDB (data not shown) or LPS (Fig. 5b) alone had no effects on the expression of M2 markers (arginase-1, YM1/2, and CD206). Notably, the combination of TDB and LPS caused a marked increase in M2-related gene expression (Fig. 5b). Further, ELISA results showed that TDB significantly increased IL-10 release in LPS-activated BV-2 cells (Fig. 5c), suggesting that TDB could promote M2 polarization of microglia. In contrast, siRNA knockdown of AMPKα attenuated TDB-induced M2 polarization of microglia, as indicated by the downregulation of IL-10 level and M2 gene expression (Fig. 5b, c). Overall, these results suggest that AMPK activation is required for TDB to induce microglial M2 polarization, but not involved in anti-inflammatory response.

Because activated microglia undergoes a shift from M1 to M2 phenotype, which is marked by alterations in central metabolic programs [35], we next investigated whether TDB can change cellular metabolism and its relationship with AMPK in LPS-stimulated cells. Treatment of BV-2 cells with TDB alone did not affect the response of mitochondrial stressors such as oligomycin, FCCP, and antimycin + rotenone (Fig. 6a, d). Nevertheless, LPS suppressed not only basal OCR (Fig. 6b) but also response of mitochondrial stressors (Fig. 6a). Respiratory capacity

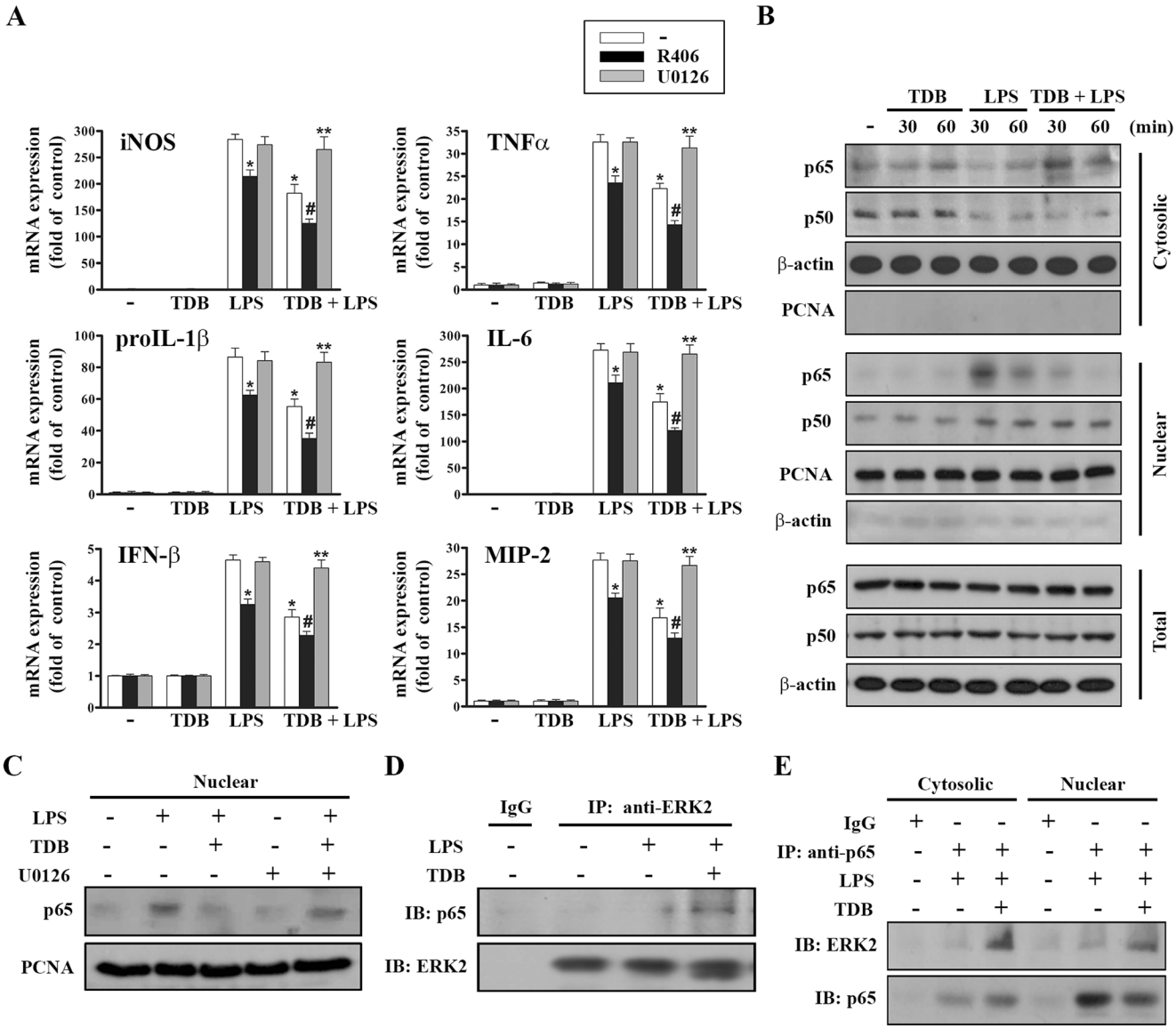

Fig. 4 *ERK activation is responsible for the anti-inflammatory action of TDB*. **a** BV-2 cells were treated with vehicle or pre-treated with either R406 (1 μM) or U0126 (10 μM) for 30 min and then treated with TDB (50 μg/ml) and/or LPS (100 ng/ml) for 5 h. Total mRNA was extracted and reversely transcribed for quantitative PCR analysis of iNOS, TNF-α, proIL-1β, IL-6, IFN-β, and MIP2 mRNA. Values were normalized to β-actin gene expression and were expressed relative to the control group. **b** After drug treatment for the indicated time intervals, nuclear translocation of NF-κB from cytosol was determined. **c** Cells were treated with vehicle or pre-treated with U0126 for 30 min before TDB and LPS stimulation. After 40 min, nuclear translocation of NF-κB was examined. **d**, **e** The association of ERK and p65 in cells with TDB and LPS stimulation was analyzed by co-immunoprecipitation using indicated antibody. Data were presented as mean ± SEM from three independent experiments. $*p < 0.05$, indicating a significant inhibition of LPS response by TDB and R406; $^{\#}p < 0.05$, indicating the additive inhibitory effects of TDB and R406 on LPS response; $**p < 0.05$, indicating a significant effect of U0126 to reverse the inhibitory actions of TDB on LPS-induced gene expression

determined under FCCP treatment was reduced after LPS stimulation, but not with TDB alone (Fig. 6c). Concomitantly, LPS shifted cell metabolism from mitochondrial oxidative phosphorylation to a glycolytic state as evidenced by increasing ECAR (Fig. 6e, f). Notably, these actions of LPS in terms of reductions in basal OCR and mitochondrial capacity but increase in glycolysis were partly reversed by co-treatment with TDB. On the other hand, knockdown of AMPK significantly potentiated LPS-mediated decreases of OCR and mitochondrial capacity (Fig. 6b, c) and increases of ECAR and glycolytic capacity (Fig. 6e, f). Under these changes upon AMPK silencing, the reversal effects of TDB on LPS responses were no longer observed. Collectively, these results suggest that LPS stimulation suppresses mitochondrial respiration and favors metabolism pathway to glycolysis, and this energy switch caused by LPS is reversed by TDB in an AMPK-dependent manner.

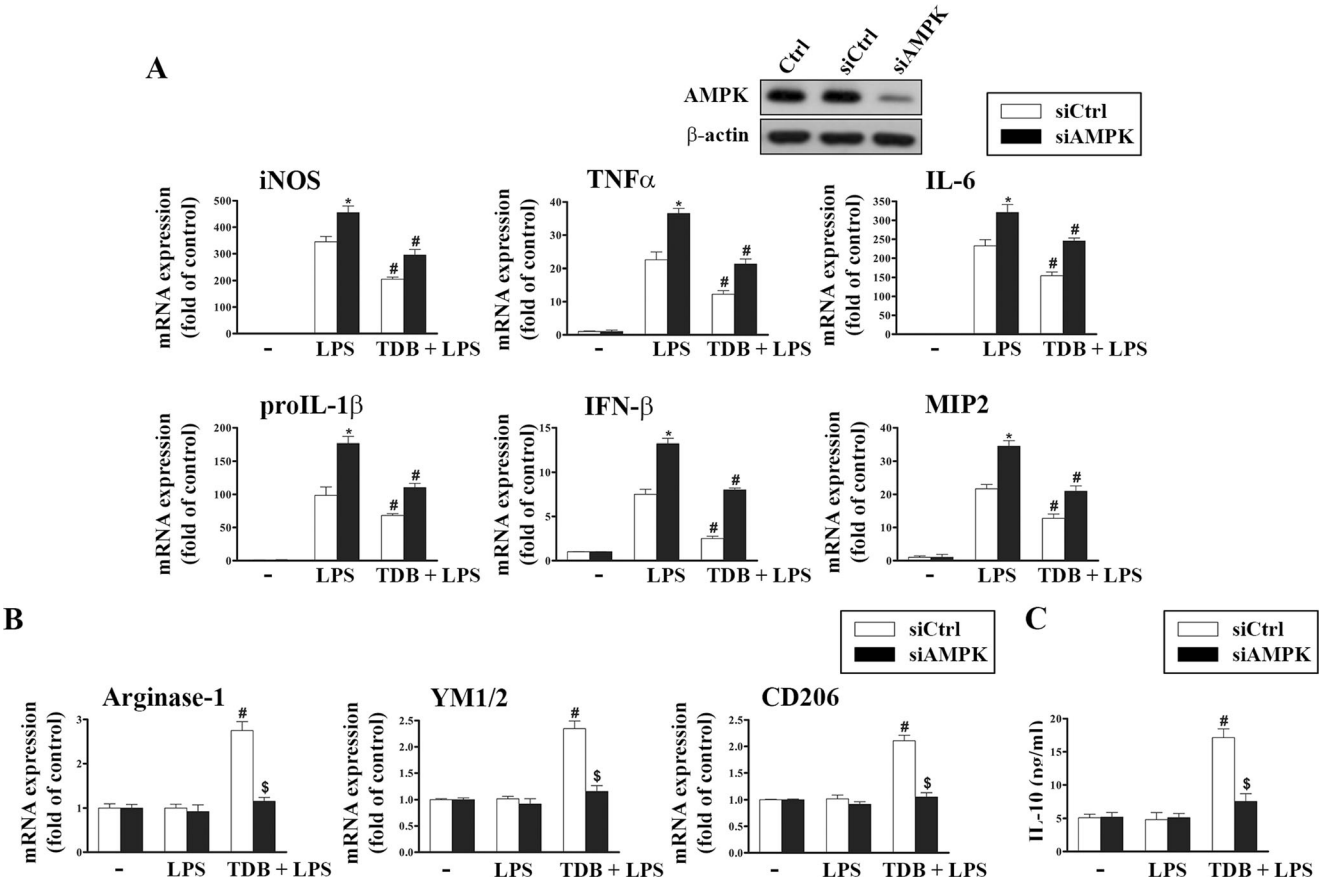

Fig. 5 *AMPK activation is involved in TDB-mediated M2 polarization of microglia.* **a** BV-2 microglia were transfected with si-Ctrl or si-AMPKα for 48 h. After siRNA transfection, total cell lysates were subjected to SDS-PAGE followed by immunoblotting. β-actin was detected as a loading control. **a**, **b** Two days post-transfection of control or AMPKα siRNA, cells were treated with vehicle or TDB (50 μg/ml) and/or LPS (100 ng/ml) for 5 h. The total mRNA was extracted and reversely transcribed for quantitative PCR analyses of M1 gene expression (**a**) and M2 markers (**b**). Values were normalized to β-actin gene expression and were expressed relative to the vehicle control group. **c** After 48 h of transfection with control or AMPKα siRNA, cells were treated with the indicated drugs for 16 h; then, the culture media were collected and analyzed for IL-10 by ELISA. Data were presented as mean ± SEM from three independent experiments. $^{*}p < 0.05$, indicating the significant increase in LPS response in si-AMPK cells; $^{\#}p < 0.05$, indicating the significant effects of TDB on LPS responses in both si-Ctrl and si-AMPK cells as well as inhibition of AMPK by si-AMPK; $^{\$}p < 0.05$, indicating a significant reversal effect of si-AMPK on the action of TDB for M2 gene expression (**b**) and IL-10 production (**c**)

TDB Inhibits LPS-Induced M1 Polarization and Promotes M2 Polarization Independent of Mincle

Mincle has been shown as an essential receptor for TDB response [21, 23, 46]. In order to investigate whether this receptor mediates the anti-inflammatory actions of TDB in microglial cells, we examined the expression of Mincle mRNA and protein levels, either in the presence or absence of TDB and/or LPS stimulation. As shown in Fig. 7a, b, TDB alone did not increase Mincle mRNA or protein levels, while LPS treatment induced a time-dependent upregulation of Mincle at both mRNA and protein levels, and these events were attenuated by TDB. Like other pro-inflammatory genes as shown in Fig. 5a, TDB inhibition of LPS-induced Mincle mRNA expression was reversed by U0126 and was additive to the effect of R406 (Fig. 7c). Furthermore, we assessed the effects of TDB on Mincle surface expression. In agreement with above findings, TDB alone had no effect on the cell surface expression of Mincle, but can suppress the LPS-induced Mincle expression on the cell surface (Fig. 7d). Previous studies demonstrate that Mincle mediates TDB-induced activation of ERK in bone marrow-derived macrophages (BMDMs) via Syk [46]. Hence, we investigated whether Mincle is involved in TDB-induced anti-inflammatory signaling in microglia. BV-2 cells were pre-treated with anti-Mincle monoclonal antibody (5 μg/ml) for 1 h before the addition of TDB and LPS. This antibody has been demonstrated to inhibit TDB-induced inflammatory responses [21]. As shown in Fig. 7e, the Mincle-neutralizing antibody did not inhibit phosphorylation of Syk, PLC-γ1, ERK1/2, p38, or JNK after treatment with TDB alone or in combination with LPS compared to the control group incubated with the isotype control antibody. Furthermore, pre-treatment with anti-Mincle did not affect LPS-induced inflammatory responses nor the TDB-induced anti-inflammatory action when compared to the control

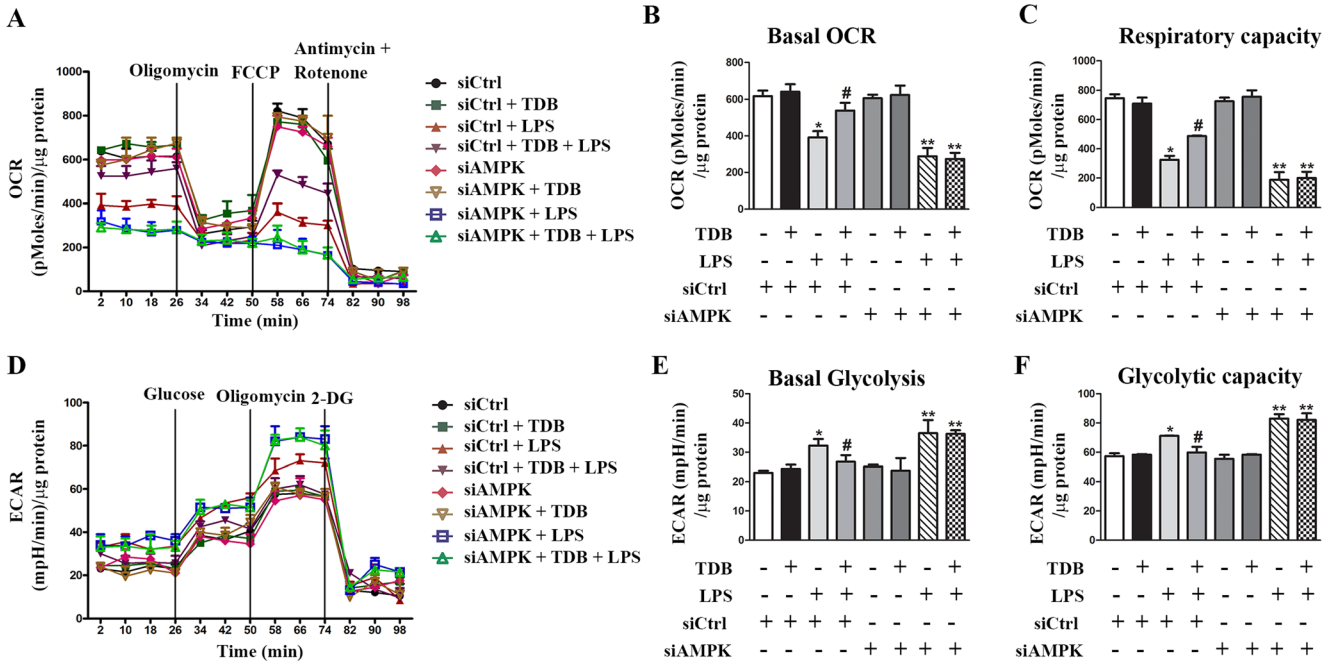

Fig. 6 *TDB reverses LPS-induced mitochondrial respiration imbalance and enhanced glycolysis*. After 48 h of transfection with si-Ctrl or AMPKα siRNA, cells were treated with vehicle or TDB (50 μg/ml) and/or LPS (100 ng/ml) for 16 h, and then, OCR (**a**) and ECAR (**d**) were measured using a seahorse XF24 extracellular flux analyzer. **b** Basal OCR was determined prior to the addition of oligomycin (2.5 μM), and **c** maximal respiratory capacity was calculated after the addition of FCCP (1 μM). **e** Basal glycolysis was determined following the addition of glucose (5.0 mM), and **f** glycolytic capacity was calculated after the addition of oligomycin (2.5 μM). Values were normalized to total protein concentration. Data were presented as mean ± SEM from three independent experiments. $^{*}p < 0.05$, indicating the significant effects of LPS; $^{\#}p < 0.05$ indicating the significant reversal effects of TDB on LPS-induced responses; $^{**}p < 0.05$, indicating the significant enhancement in response to LPS either alone or in combination with TDB in AMPK-silenced cells

(Fig. 7f). Likewise, anti-Mincle antibody did not block TDB-induced M2 markers (Fig. 7g) nor IL-10 production (Fig. 7h). Together, these data indicate that the anti-inflammatory effects of TDB are Mincle independent.

Mincle Knockout Does Not Affect TDB-Induced Inhibition of M1 Polarization and Promotion of M2 Polarization in Primary Microglia

To further confirm our findings in BV-2 cells that TDB elicits the Mincle-independent actions to inhibit inflammatory responses and promote M2 polarization, we examined both events again in primary microglial cells isolated from WT and Mincle$^{-/-}$ mice. Similar to that observed in BV-2 cells, TDB treatment alone for 30 min caused a significant increase in ERK1/2 phosphorylation and a slight activation of p38 in both WT and Mincle$^{-/-}$ cells (Fig. 8a). As expected, LPS treatment resulted in the same extents of signaling events in WT and Mincle$^{-/-}$ cells, including degradation of IκBα and activation of p38, JNK, and IKKα/β (Fig. 8a). Similarly, TDB and LPS co-treatment synergistically enhanced ERK1/2 and AMPK phosphorylation in WT and Mincle$^{-/-}$ primary microglia.

Next, we investigated the effects of TDB on LPS-induced expression of pro-inflammatory cytokines in WT and Mincle$^{-/-}$ primary microglia. Treatment with LPS alone for 5 h induced marked increases in M1 gene expression like COX-2, iNOS, TNF-α, proIL-1β, IL-6, MIP2, IFN-β, and Mincle (Fig. 8b), but failed to change M2 signature gene expression like arginase-1, YM1/2, and CD206 (Fig. 8c). Upon TDB co-treatment, the upregulated M1 gene expression by LPS except COX-2 was attenuated, while M2 gene expression was oppositely enhanced (Fig. 8b, c). It is interesting to note that although the effects of LPS were not altered in Mincle$^{-/-}$ microglia as compared to the WT group, the TDB-induced inhibition of inflammatory genes and enhancement of M2 genes were more apparent in Mincle$^{-/-}$ microglia (Fig. 8b, c). The ELISA results further revealed that TDB significantly increased protein production of anti-inflammatory cytokine IL-10 in LPS-stimulated Mincle$^{-/-}$ microglia compared with WT microglia (Fig. 8d). Altogether, these data suggest that TDB can inhibit inflammatory responses and promotes M2 polarization in primary microglial cells and both actions of TDB are independent of Mincle.

TDB Suppresses Microglia-Mediated Neurotoxicity in a Mincle-Independent Manner

Several studies have demonstrated that persistent activation of microglia can be neurotoxic to neighboring neurons by

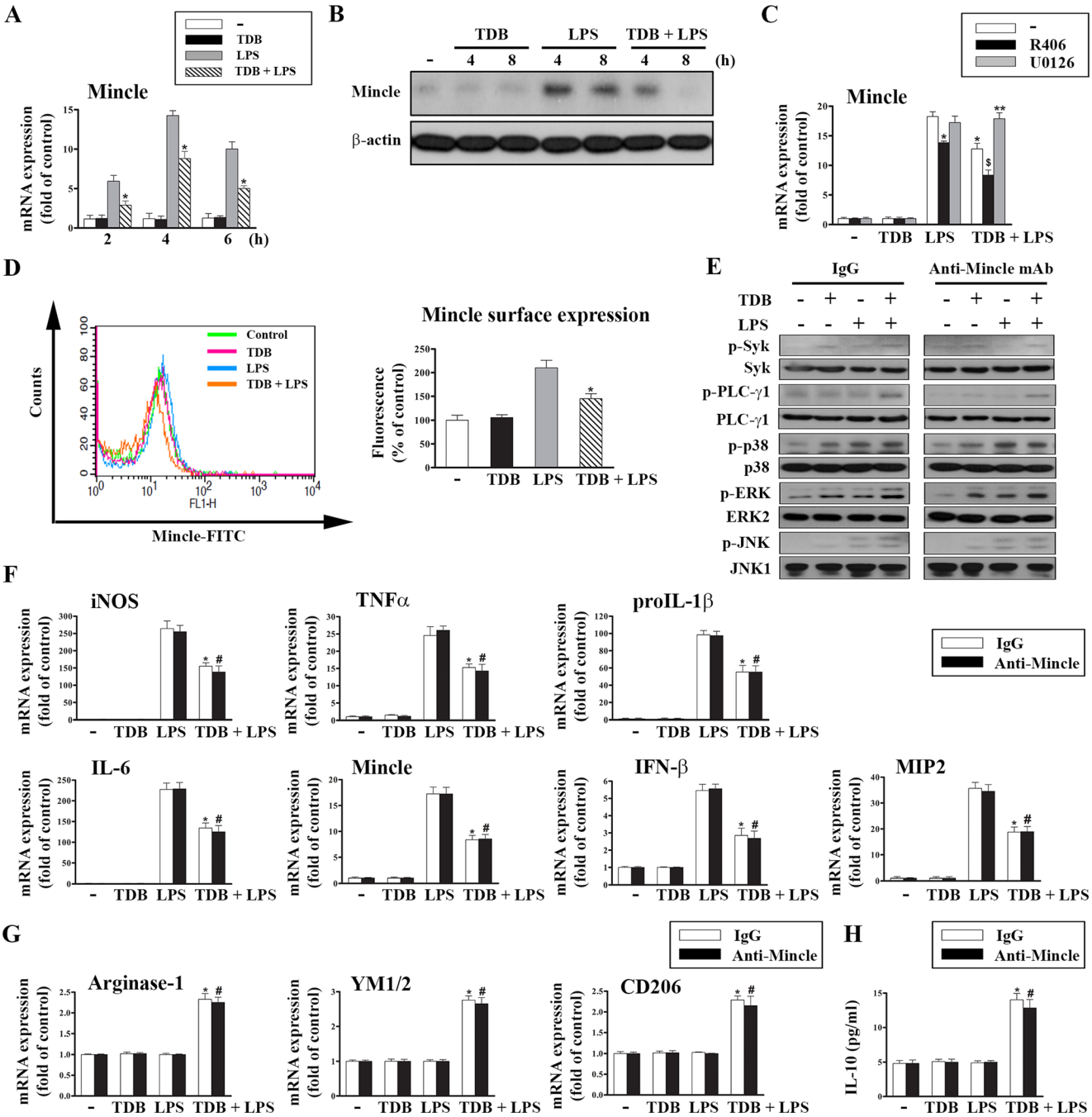

Fig. 7 *TDB suppresses LPS-induced M1 polarization and promotes M2 polarization of microglia independent of Mincle*. BV-2 cells were treated with vehicle or TDB (50 μg/ml) and/or LPS (100 ng/ml) for different time periods as indicated (**a**, **b**), 1 h (**e**), or 5 h (**c**, **f**, **g**). Gene and protein expressions were determined by quantitative PCR (**a**, **c**, **f**, **g**) and immunoblotting (**b**, **e**) respectively. In some experiments, cells were treated with vehicle control or pre-treated with R406 (1 μM) or U0126 (10 μM) for 30 min (**c**), or with 5 μg/ml control IgG (IgG) or Mincle-neutralizing antibody (Ab) for 1 h (**e**–**h**). For measuring surface Mincle expression (**d**), after treatment with vehicle or TDB (50 μg/ml) and/or LPS (100 ng/ml) for 5 h, cells were incubated with anti-mouse Mincle and analyzed for Mincle cell surface expression by flow cytometry, and quantitative data were determined. **h** After 16 h of treatment with the indicated drugs, the culture supernatant was collected and analyzed for IL-10 protein levels by ELISA. Data were presented as mean ± SEM from three independent experiments. $^{*}p < 0.05$, indicating significant effects of TDB and R406 on LPS-induced responses; $^{\$}p < 0.05$, indicating the additive inhibitory effects of TDB and R406 on LPS response; $^{**}p < 0.05$, indicating the significant effect of U0126 to reverse the inhibitory actions of TDB on LPS-induced gene expression; $^{\#}p < 0.05$, indicating no significant effect of anti-Mincle antibody on the actions of TDB

releasing toxic molecules, such as pro-inflammatory cytokines and NO [32, 47]. Thus, we investigated whether the inhibition of M1 microglial polarization while promoting M2 microglial polarization by TDB can protect neurons. To

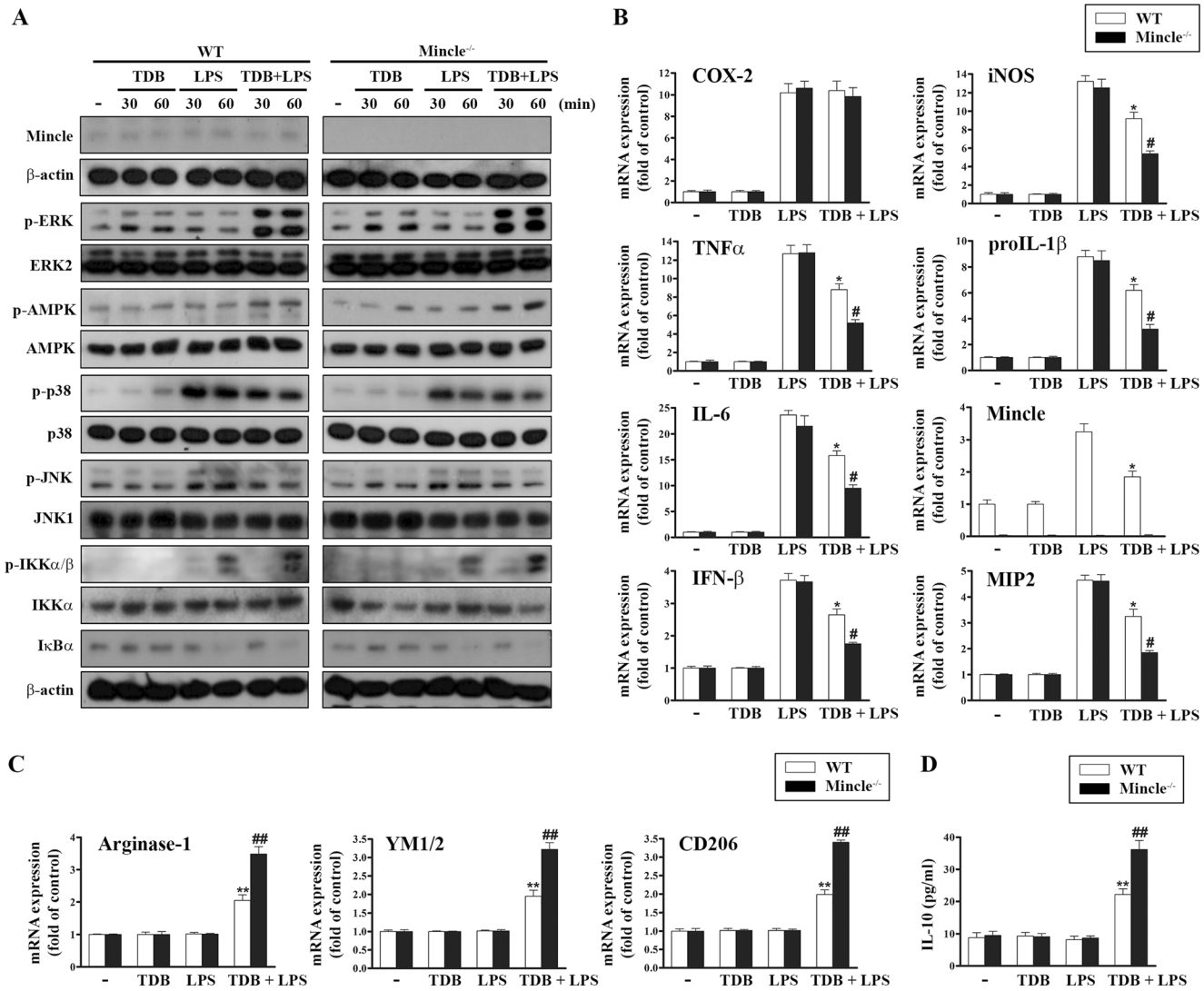

Fig. 8 *Mincle silencing enhances TDB actions in the inhibition of inflammatory gene expression and promotes microglial polarization towards M2 phenotype*. Primary microglia from WT and Mincle$^{-/-}$ were treated with vehicle or TDB (50 μg/ml) and/or LPS (100 ng/ml) for different time periods as indicated (**a**), 5 h (**b**, **c**), or 16 h (**d**). Total cell lysates were subjected to SDS-PAGE followed by Western blot analysis (**a**). The total mRNA was extracted and reversely transcribed for quantitative PCR analysis of M1 and M2 gene expression (**b**, **c**). In **d**, after treatment, the culture media were collected and IL-10 levels were determined by ELISA. Data were presented as mean ± SEM from three independent experiments. $^{*}p < 0.05$, indicating the significant effects of TDB on LPS responses in WT primary microglia; $^{\#}p < 0.05$, indicating the significant enhancement of TDB actions in LPS-stimulated Mincle$^{-/-}$ cells as compared to WT primary microglia

this end, we collected microglia-derived conditioned media (MCM) of BV-2 cells after treatment with LPS and/or TDB. We found LPS-MCM can induce a 35% decrease in cell viability in human neuroblastoma SH-SY5Y cells, while TDB/LPS-MCM had no effect (Fig. 9a). Furthermore, we also verified this effect in primary cortical neurons and microglia prepared from WT and Mincle$^{-/-}$ mice. We found MCM of primary microglia (p-MCM) collected from both LPS-treated WT and Mincle$^{-/-}$ microglia were toxic to cortical neurons of WT and Mincle$^{-/-}$, and this effect was attenuated when p-MCM were from microglial cells co-treated with LPS and TDB (Fig. 9b). Notably, a more prominent protective effect of p-MCM elicited by TDB was observed in Mincle$^{-/-}$ than WT microglia. Conversely, TDB did not protect human SH-SY5Y cells and mouse primary cortical neurons against the direct toxicity of H_2O_2 (Fig. 9c). Collectively, these results imply that TDB might exert the neuroprotection by indirect inhibition of pro-inflammatory microglial activation through a mechanism independent of Mincle.

TDB Attenuates Neuroinflammatory Response in LPS-Injected Mice Independent of Mincle

After observing the anti-inflammatory effect of TDB in microglial cells, we further evaluate this action in a mouse model of neuroinflammation. We administered LPS and

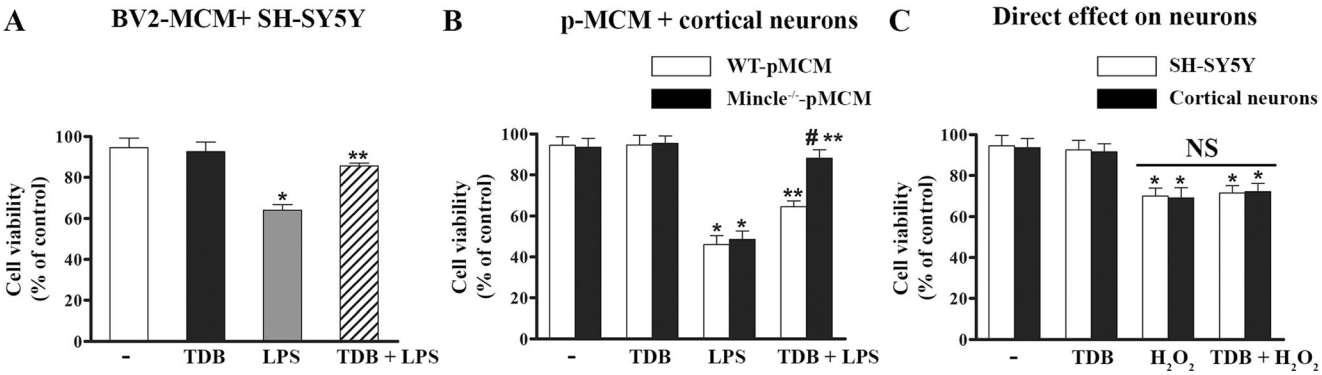

Fig. 9 *TDB protects neurons against microglia-mediated cytotoxicity.* **a** SH-SY5Y cells were treated with microglial conditional media (MCM) from BV-2 cells for 24 h. **b** WT primary cortical neurons were incubated for 24 h with primary microglial conditional media (p-MCM) collected from either WT or Mincle$^{-/-}$ primary microglia that were exposed to TDB (50 μg/ml) and/or LPS (100 ng/ml) for 5 h followed by 24 h of incubation in fresh media. **c** SH-SY5Y and WT primary cortical neurons were exposed to H_2O_2 (300 μg/ml) in the presence or absence of TDB (50 μg/ml) for 24 h. MTT assay was performed to determine the neuronal viability. Data were presented as mean ± SEM from three independent experiments.*$p < 0.05$, indicating a significant decrease of neuronal viability by MCM from LPS-treated BV-2 cells (**a**), p-MCM from LPS-treated WT and Mincle$^{-/-}$ primary microglia (**b**), or H_2O_2 (**c**); **$p < 0.05$, indicating the significant effect of MCM from TDB/LPS-co-treated microglial cells to reverse the actions of LPS in cell death; $^{\#}p < 0.05$, indicating the higher protective effect of TDB in Mincle$^{-/-}$ p-MCM than WT p-MCM. NS, non-significance

TDB intraperitoneally to mice in a 7-day regimen as shown in Fig. 10a. We found that LPS treatment increased the Iba-1 (microglia activation marker) level in the hippocampus and cerebellum of both WT and Mincle$^{-/-}$ mice (Fig. 10b). Interestingly, TDB administration significantly attenuated Iba-1 expression caused by LPS in both WT and Mincle$^{-/-}$ mice (Fig. 10b). Inhibition of microglia-mediated neuroinflammation by TDB was further supported by the decreased LPS-induced pro-inflammatory markers in the hippocampus, except COX-2 in the cerebellum of WT and Mincle$^{-/-}$ mice (Fig. 10c, d). In addition, TDB and LPS co-administration can increase arginase-1 protein expression in both the hippocampus and cerebellum of WT and Mincle$^{-/-}$ mice (Fig. 10e). Taken together, these results suggest that TDB suppresses microglia-mediated neuroinflammation through a Mincle-independent mechanism.

Pro-inflammatory cytokines in the brain are partially responsible for changes in behavioral responses (e.g., anorexia and decreased locomotors activity). We therefore assessed the effects of TDB on sickness behavior in WT and Mincle$^{-/-}$ mice following peripheral LPS injection. We found that TDB alone did not affect food intake (Fig. 10f), body weight (Fig. 10g), and locomotor activity in WT and Mincle$^{-/-}$ mice. The latter was assessed by open-field test, indexed by either line crossing (Fig. 10h) or rearing (Fig. 10i). In contrast, LPS administration led to significant decreases in food consumption, body weight, and locomotor activities in both genotype mice. These changes caused by LPS were significantly attenuated by TDB in WT mice. More surprisingly, TDB-induced restoration of these behavior responses of LPS was much more apparent in Mincle$^{-/-}$ mice as compared to WT mice (Fig. 10f–i). All these data not only indicate the ability of TDB to attenuate LPS-elicited inflammation and sickness behavior through a Mincle-independent mechanism but also suggest the existence of a Mincle-dependent factor to deteriorate disease severity upon TDB and LPS co-administration.

Discussion

In this study, we unexpectedly found that TDB can attenuate LPS-induced inflammatory responses in microglial cells and mouse brain. Our data indicate that this action is consequential of at least two bifurcated signaling pathways driven by TDB and LPS together, i.e., PLC-γ1 activation coupling to PKC/ERK and Ca^{2+}/CaMKKβ/AMPK pathways. The former leads to inhibition of the p65 nuclear translocation and NF-κB/p65-driven inflammatory gene expression. The latter leads to M2 polarization of microglia and enhancement in mitochondrial bioenergetics. Moreover, for the first time, we provide evidence for a novel Mincle-independent anti-inflammatory action of TDB in microglia and brain.

In microglial cells, we found insufficient signaling events for TDB alone to induce proinflammatory response even after incubating the cells with TDB for 48 h (data not shown). This observation is unlike TDB action in macrophages, dendritic cells, and mast cells where it can activate Mincle and induce Syk-dependent signaling cascades via FcRγ including PLCγ, NF-κB, ERK, and/or PKCσ for inflammatory gene expression [22, 42, 46]. Previous studies have shown that BMDMs can be stimulated by TDB alone when either coating or suspension manner was used. To elucidate if different treatment manner is related to the distinct actions of TDB between BMDMs and microglia, we also used coating manner in BMDMs and BV-2 cells. We found that stimulation of BMDMs with TDB alone either in suspension or plate-bound form induces expression

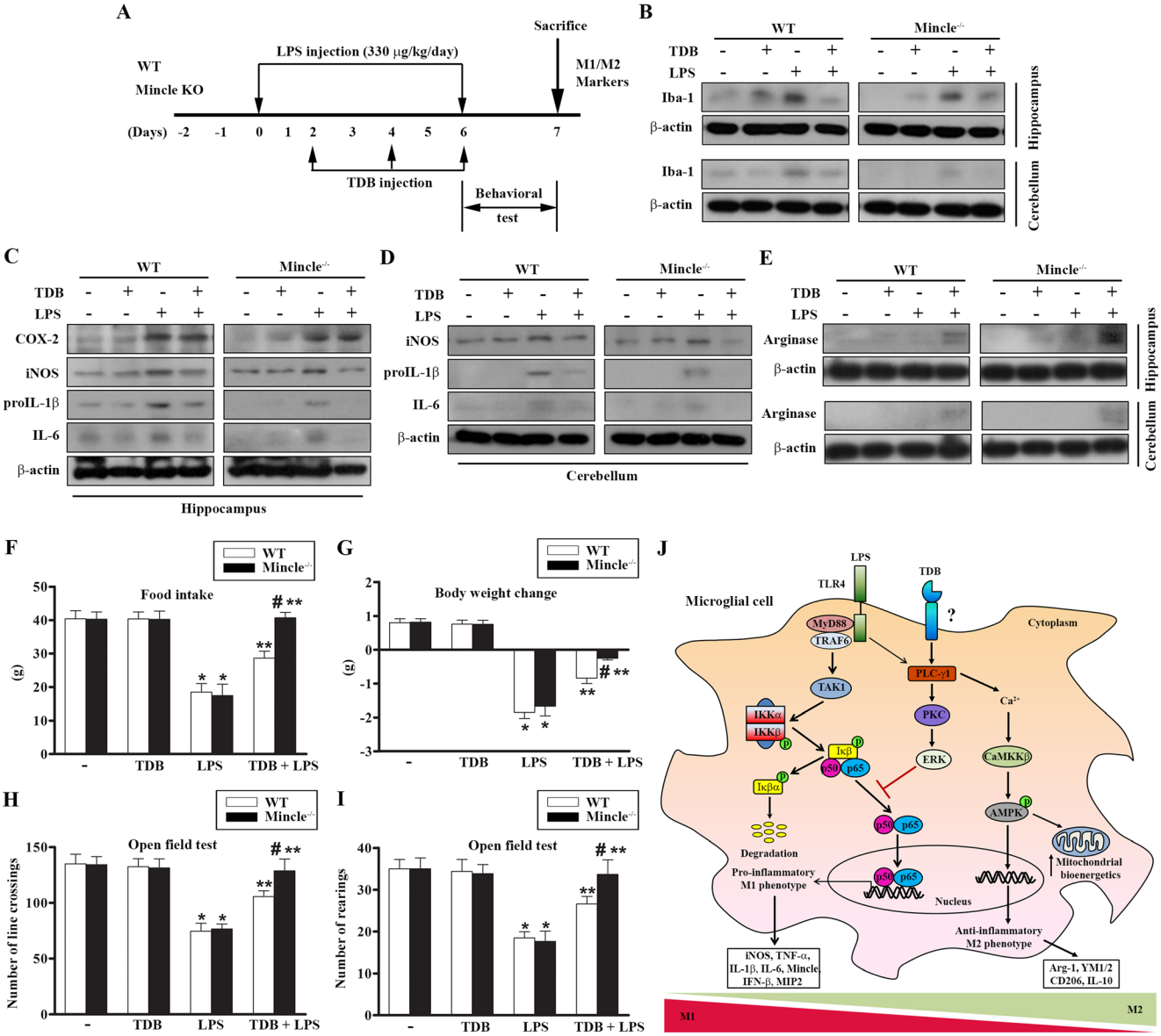

Fig. 10 *TDB switches microglial M1/M2 polarization and ameliorates sickness behavior in LPS-challenged mice.* **a** Experimental timeline in mice. WT and Mincle$^{-/-}$ mice were injected intraperitoneally with 330 μg/kg LPS once daily for 7 days. TDB (50 μg/mouse) was administered intraperitoneally alone or together with LPS at days 2, 4, and 6. After injection, mouse behavioral tests were performed at day 6 before they were killed on day 7. The hippocampus and cerebellum were harvested and immediately frozen in liquid nitrogen and stored at − 80 °C until further analyses. Protein levels of Iba-1 (**b**), M1 gene expression (**c**, **d**), and M2 marker arginase-1 (**e**) in the hippocampus and cerebellum were determined by immunoblotting analysis. At day 6, food intake (**f**), body weight (**g**), and locomotor activity (**h**, **i**) were measured. **j** Proposed model for the molecular mechanism of TDB to inhibit LPS-induced inflammatory response and promote microglial polarization towards M2 phenotype. In microglial cells, TDB acting through an unidentified receptor triggers PLC-γ1 signaling pathway, leading to the activation of PKC and mobilization of intracellular calcium level. The former induces ERK activation that in turn blocks NF-κB nuclear translocation and pro-inflammatory gene expression. The latter activates CaMKKβ and AMPK that in turn promote M2 microglial polarization and increase mitochondrial bioenergetic function. Data were presented as mean ± SEM from five independent experiments. *$p < 0.05$, indicating significant effects of LPS in behavioral responses; **$p < 0.05$, indicating significant effects of TDB to reverse the actions of LPS in WT and Mincle$^{-/-}$ mice; $^{\#}p < 0.05$, indicating the more significant reversal effect of TDB on the response of LPS in Mincle$^{-/-}$ than WT mice

of pro-inflammatory cytokines such as COX-2, iNOS, IL-1β, IL-6, Mincle, IFN-γ, and MIP2 (Supplementary Fig. 2B). In contrast, TDB of both treatment forms did not have any effects on inflammatory gene expression in BV-2 cells even after 48-h incubation (Supplementary Fig. 2A). The latter effects are consistent to our findings by treating BV-2 cells with TDB alone in suspension manner for 2 and 5 h (Fig. 1d). Therefore, we conclude that TDB alone did not induce response in BV-2 cells which is different from that in other immune cells.

Supporting this unique finding in microglial cells, our data surprisingly reveal the anti-inflammatory actions of TDB via a

mechanism independent of Mincle and Syk. Currently, the role of Mincle in neuroinflammation is still limited. Even though Mincle and Syk have been suggested to play an important role in the pathogenesis of ischemic stroke [24], our current data using neutralizing Mincle antibody which has been shown to block Mincle [21] and genetic knockout approach in Mincle$^{-/-}$ cells and mice to exclude the involvement of Mincle in TDB-elicited anti-neuroinflammatory actions. Previously, TDB inhibition of LPS response in splenocytes is proved to be through Mincle receptor [48]. We assume that the Mincle-independent action of TDB in microglia might be due to very weak expression of this receptor at resting microglial cells as compared to BMDMs [46]. Similar findings were reported for limited expression of Mincle in both primary microglia [49] and BV-2 cells [27] at basal culture condition. Here, we also confirmed these findings in our study as shown in Fig. 8a for primary microglia and in Fig. 7b for BV-2 cells.

In agreement with previous notion that Mincle is an NF-κB target gene [50], we show the ability of LPS to upregulate Mincle expression in BV-2 and primary microglia. At present, there is no direct evidence to identify the targeted receptor(s) of TDB in microglia to trigger signaling pathways for the anti-inflammatory response. However, the possible involvement of Mcl in this action needs further investigation. Mcl is a co-receptor of TDB, which is constitutively expressed in myeloid cells. It functions as an initial sensor to recognize TDM and trigger Mincle expression in a CARD9/BCL10/MALT1-dependent NF-κB activation manner [51]. Our results demonstrate that CARD9, the central adaptor protein, is not involved in TDB-induced ERK signaling (data not shown). Another interesting finding in this study is the stronger protective effect of TDB against LPS-induced neuroinflammation in Mincle$^{-/-}$ microglial cells and mice. These findings imply the existence of Mincle-mediated inflammatory actions under the condition of TDB and LPS co-treatment. We suggest this event might be due to the increased Mincle expression by LPS via NF-κB signal and subsequent activation by TDB for enhanced inflammation.

In microglia, we found that the signaling pathways triggered by TDB or LPS alone are largely different but additive. TDB-induced a rapid and transient phosphorylation of Syk, ERK, p38, and JNK in microglial cells, but not the most essential signal required for inflammatory gene transcription, i.e., IKK-dependent NF-κB activation. In this study, we demonstrate a Syk-independent additive action of TDB and LPS to activate PLC-γ1 and downstream signaling pathways. Even though Syk is a common and key upstream signaling molecule for immune receptors and CLRs, and has been shown to induce PLC-γ1 activation [52, 53], we rule out this action in TDB-treated microglia. We suggest this differential phenomenon might be due to an unidentified target of TDB instead of Mincle in microglia as we discussed above. Therefore, it is interesting for us to further determine the Syk-mediated downstream signals and cellular responses in TDB-treated microglia in the future. Of note, we found PLC-γ1 activation contributes to the anti-inflammatory action in microglia. Unlike other cell types, e.g., mast cells, PLC-γ mediates ERK and calcium signals for cell activation and gene regulation [42]. PLC-γ1 activation was shown to inhibit LPS-induced inflammatory response in microglia [54]. Here, we further demonstrate the branched signaling pathways downstream PLC-γ1 to induce anti-inflammatory and M2 polarization in microglia through PKC/ERK and CaMKK/AMPK, respectively.

More interestingly, LPS can also activate Syk in BV-2 cells, and similar results were observed in LPS-stimulated macrophages [55] and dendritic cells [40, 56]. Nevertheless, the effects of R406 on LPS-induced signaling pathways and up-regulation of inflammatory gene expression in BV-2 are unlike our previous findings in BMDM [33]. In BV-2 cells, R406 decreased LPS/TDB-induced p38 and JNK activities, while it had no effects on IKK, PLC-γ1, or PKC activity. Moreover, our data also show the ability of R406 to increase ERK1/2 activation in BV-2 cells in response to TDB, LPS, or LPS/TDB. Accordingly, LPS-induced inflammatory gene transcription which completely relies on the p38 and JNK activities was reduced by R406. In contrast, LPS-induced IKK, JNK, and p38 activities via MyD88 as well as multiple inflammatory gene responses in BMDM were enhanced by R406 and Syk knockout [33]. Moreover, Syk also mediates a negative role in TLR4-mediated inflammatory responses in macrophages [57]. All these results suggest the distinct but cell context-specific manner of TLR4 signaling in macrophages and microglia.

Currently, the signaling interplay of MEK/ERK and NF-κB pathways still remains elusive and complicated. ERK can mediate NF-κB activation via IκBα p65 phosphorylation and degradation [58, 59]. Nevertheless, opposite findings were also demonstrated that ERK negatively regulates NF-κB-dependent gene expressions [60, 61]. Moreover, MEK-ERK activation leads to the protein interaction of p65 and ERK, and in turn a decreased nuclear translocation of both molecules [62]. Our current data support a negative regulatory role of ERK in classical NF-κB activation triggered by TLR4 in microglial cells. The NF-κB inhibition by TDB accounts for the decrease in expression of many pro-inflammatory genes induced by LPS. Nevertheless, the expression level of COX-2 is not altered by TDB. We suggest such difference is because NF-κB is dispensable for COX-2 promoter activation [63]. Vice versa, CREB, ATF, and c/EBPs are essential for optimal COX-2 expression [64].

An emerging concept is that inflammation may involve in the control of metabolic reprogramming and functional phenotypes of immune cells including microglia [35]. Polarization of M1 phenotype is often accompanied by a shift in cells from oxidative phosphorylation to aerobic

glycolysis for energy production. AMPK is a heterotrimeric serine/threonine kinase that acts as a sensor of cellular energy, being activated by various types of stress including low ATP:AMP ratios, Ca^{2+}/CaMKKβ, and LKB [65]. AMPK has been shown to link cellular metabolism and inflammation in various cell types including microglial cells, thus playing an important role in the regulation of neuroinflammation and pathogenesis of CNS diseases [66, 67]. Previous studies reported that several AMPK activators can significantly suppress pro-inflammatory cytokine production and tissue inflammatory destruction [68, 69]. Recently, AMPK activation was shown to promote M2 microglia/macrophage polarization and inhibit inflammatory response [29, 70]. Our current data indicate the contribution of AMPK activation synergized by TDB and LPS treatment to M2 polarization and mitochondrial energy production in microglia. Basal AMPK activity can back up the mitochondrial respiration and attenuate energy source from glycolysis in LPS-stimulated microglial cells. Increased AMPK activity upon TDB and LPS co-treatment is also required for the energy balancing and M2 polarization effects of TDB. Thus, both actions of AMPK support it as a therapeutic target for the treatment of neuroinflammatory diseases.

Systemic administration of LPS has been shown to activate microglia and induce sickness behavior, including anorexia, reduced locomotor activity, and weight loss [39]. In this study, we found that the administration of TDB can attenuate LPS-induced inflammatory responses and promote microglial M2 polarization in the hippocampus and cerebellum of both WT and Mincle$^{-/-}$ mice. Although, previous in vivo studies have demonstrated the roles of Mincle in macrophage polarization to M1 and the pathological outcome in ischemic stroke [24, 50], our results rule out the contribution of Mincle in the CNS action of TDB. Surprisingly, we demonstrate that TDB administration can recover the LPS-induced sickness behavior more apparently in Mincle$^{-/-}$ compared with WT mice, while the loss of Mincle had no change in LPS-induced sickness behavior. These results further support our in vitro findings in microglia as mentioned above and suggest a pathological role of Mincle in the brain when microglial Mincle expression is upregulated by LPS followed by activation via TDB. Besides this possible explanation for the unexpected in vivo findings in Mincle$^{-/-}$ mice, another possibility is the suggestion from an ischemic stroke study. As reported, an atypical role of Mincle in a subset of macrophages resident in the perivascular niche is suggested to be the crucial regulator of a poor outcome following transient middle cerebral artery occlusion [49]. In addition, our data do not exclude indirect effects of TDB on other target cells, such as neurons. We found that TDB exerts neuroprotective effects independent of Mincle via suppressing microglial activation and subsequent neuronal cell death. Overall, our results indicate that TDB can inhibit LPS-induced pro-inflammatory responses and protect microglia-induced neurotoxicity in a Mincle independent manner.

In summary, we demonstrated a novel molecular mechanism for the interaction between TDB, the cord factor synthetic analogue of *Mtb*, and LPS. TDB can induce Mincle- and Syk-independent actions to antagonize TLR4-mediated inflammatory responses in microglia. Upon TDB and LPS co-treatment, an enhanced PLC-γ1 activation leads to downstream bifurcated signaling pathways of PKC/ERK and Ca^{2+}/CaMKK/AMPK. In turn, the former signaling interferes with LPS-induced NF-κB activation and inflammatory gene expression. The latter signaling shifts LPS-stimulated cells into M2 polarization and enhances mitochondrial energy metabolism (Fig. 10j). These findings provide new insights into TDB for its novel anti-inflammatory action mechanisms in microglia and therapeutic potential in neurodegenerative disorders.

Acknowledgements We thank Dr. Shie-Liang Hsieh (Genomics Research Center, Academia Sinica, Taipei, Taiwan) for Mincle$^{-/-}$ mice and Dr. Wen-Mei Fu (Department of Pharmacology, College of Medicine, National Taiwan University, Taipei, Taiwan) for providing SH-SY5Y cells.

Funding Information This study was financially supported by the Ministry of Science and Technology, Taiwan (MOST 103-2320-B-002-069-MY3; 106-2321-B-002-021) and National Taiwan University Hospital (UN107-032).

Compliance with Ethical Standards

The study was approved by the National Taiwan University College of Medicine Ethics Committee in accordance with their guidelines for the care of animals (protocol no. 20110047).

Conflict of Interest The authors declare that they have no competing interests.

References

1. Prinz M, Priller J (2014) Microglia and brain macrophages in the molecular age: from origin to neuropsychiatric disease. Nat Rev Neurosci 15(5):300–312. https://doi.org/10.1038/nrn3722
2. Glass CK, Saijo K, Winner B, Marchetto MC, Gage FH (2010) Mechanisms underlying inflammation in neurodegeneration. Cell 140(6):918–934. https://doi.org/10.1016/j.cell.2010.02.016
3. Casano AM, Peri F (2015) Microglia: multitasking specialists of the brain. Dev Cell 32(4):469–477. https://doi.org/10.1016/j.devcel.2015.01.018
4. Saijo K, Glass CK (2011) Microglial cell origin and phenotypes in health and disease. Nat Rev Immunol 11(11):775–787. https://doi.org/10.1038/nri3086
5. Hu X, Leak RK, Shi Y, Suenaga J, Gao Y, Zheng P, Chen J (2015) Microglial and macrophage polarization-new prospects for brain repair. Nat Rev Neurol 11(1):56–64. https://doi.org/10.1038/nrneurol.2014.207

6. Xu L, He D, Bai Y (2016) Microglia-mediated inflammation and neurodegenerative disease. Mol Neurobiol 53(10):6709–6715. https://doi.org/10.1007/s12035-015-9593-4
7. Centers for Disease C, Prevention (2012) Global routine vaccination coverage, 2011. MMWR Morb Mortal Wkly Rep 61(43):883–885
8. Rodrigues LC, Diwan VK, Wheeler JG (1993) Protective effect of BCG against tuberculous meningitis and miliary tuberculosis: a meta-analysis. Int J Epidemiol 22(6):1154–1158
9. Brenner SR (2014) Effects of Bacille Calmette-Guerin after the first demyelinating event in the CNS. Neurology 83(4):380–381. https://doi.org/10.1212/01.wnl.0000452678.33365.c7
10. Lacan G, Dang H, Middleton B, Horwitz MA, Tian J, Melega WP, Kaufman DL (2013) Bacillus Calmette-Guerin vaccine-mediated neuroprotection is associated with regulatory T-cell induction in the 1-methyl-4-phenyl-1,2,3,6-tetrahydropyridine mouse model of Parkinson's disease. J Neurosci Res 91(10):1292–1302. https://doi.org/10.1002/jnr.23253
11. Zuo Z, Qi F, Yang J, Wang X, Wu Y, Wen Y, Yuan Q, Zou J et al (2017) Immunization with Bacillus Calmette-Guerin (BCG) alleviates neuroinflammation and cognitive deficits in APP/PS1 mice via the recruitment of inflammation-resolving monocytes to the brain. Neurobiol Dis 101:27–39. https://doi.org/10.1016/j.nbd.2017.02.001
12. Lee J, Reinke EK, Zozulya AL, Sandor M, Fabry Z (2008) Mycobacterium bovis bacille Calmette-Guerin infection in the CNS suppresses experimental autoimmune encephalomyelitis and Th17 responses in an IFN-gamma-independent manner. J Immunol 181(9):6201–6212
13. Yang J, Qi F, Gu H, Zou J, Yang Y, Yuan Q, Yao Z (2016) Neonatal BCG vaccination of mice improves neurogenesis and behavior in early life. Brain Res Bull 120:25–33. https://doi.org/10.1016/j.brainresbull.2015.10.012
14. Li Q, Zhang Y, Zou J, Qi F, Yang J, Yuan Q, Yao Z (2016) Neonatal vaccination with bacille Calmette-Guerin promotes the dendritic development of hippocampal neurons. Hum Vaccin Immunother 12(1):140–149. https://doi.org/10.1080/21645515.2015.1056954
15. Yang J, Qi F, Yao Z (2016) Neonatal Bacillus Calmette-Guerin vaccination alleviates lipopolysaccharide-induced neurobehavioral impairments and neuroinflammation in adult mice. Mol Med Rep 14(2):1574–1586. https://doi.org/10.3892/mmr.2016.5425
16. Geisel RE, Sakamoto K, Russell DG, Rhoades ER (2005) In vivo activity of released cell wall lipids of Mycobacterium bovis bacillus Calmette-Guerin is due principally to trehalose mycolates. J Immunol 174(8):5007–5015
17. Fujita Y, Naka T, McNeil MR, Yano I (2005) Intact molecular characterization of cord factor (trehalose 6,6′-dimycolate) from nine species of mycobacteria by MALDI-TOF mass spectrometry. Microbiology 151(Pt 10):3403–3416. https://doi.org/10.1099/mic.0.28158-0
18. Hunter RL, Olsen MR, Jagannath C, Actor JK (2006) Multiple roles of cord factor in the pathogenesis of primary, secondary, and cavitary tuberculosis, including a revised description of the pathology of secondary disease. Ann Clin Lab Sci 36(4):371–386
19. van Dissel JT, Joosten SA, Hoff ST, Soonawala D, Prins C, Hokey DA, O'Dee DM, Graves A et al (2014) A novel liposomal adjuvant system, CAF01, promotes long-lived Mycobacterium tuberculosis-specific T-cell responses in human. Vaccine 32(52):7098–7107. https://doi.org/10.1016/j.vaccine.2014.10.036
20. Roman VR, Jensen KJ, Jensen SS, Leo-Hansen C, Jespersen S, da Silva Te D, Rodrigues CM, Janitzek CM et al (2013) Therapeutic vaccination using cationic liposome-adjuvanted HIV type 1 peptides representing HLA-supertype-restricted subdominant T cell epitopes: safety, immunogenicity, and feasibility in Guinea-Bissau. AIDS Res Hum Retrovir 29(11):1504–1512. https://doi.org/10.1089/AID.2013.0076
21. Ishikawa E, Ishikawa T, Morita YS, Toyonaga K, Yamada H, Takeuchi O, Kinoshita T, Akira S et al (2009) Direct recognition of the mycobacterial glycolipid, trehalose dimycolate, by C-type lectin Mincle. J Exp Med 206(13):2879–2888. https://doi.org/10.1084/jem.20091750
22. Strasser D, Neumann K, Bergmann H, Marakalala MJ, Guler R, Rojowska A, Hopfner KP, Brombacher F et al (2012) Syk kinase-coupled C-type lectin receptors engage protein kinase C-sigma to elicit Card9 adaptor-mediated innate immunity. Immunity 36(1):32–42. https://doi.org/10.1016/j.immuni.2011.11.015
23. Werninghaus K, Babiak A, Gross O, Holscher C, Dietrich H, Agger EM, Mages J, Mocsai A et al (2009) Adjuvanticity of a synthetic cord factor analogue for subunit Mycobacterium tuberculosis vaccination requires FcRγ-Syk-Card9-dependent innate immune activation. J Exp Med 206(1):89–97. https://doi.org/10.1084/jem.20081445
24. Suzuki Y, Nakano Y, Mishiro K, Takagi T, Tsuruma K, Nakamura M, Yoshimura S, Shimazawa M et al (2013) Involvement of Mincle and Syk in the changes to innate immunity after ischemic stroke. Sci Rep 3:3177. https://doi.org/10.1038/srep03177
25. He Y, Xu L, Li B, Guo ZN, Hu Q, Guo Z, Tang J, Chen Y et al (2015) Macrophage-inducible C-type lectin/spleen tyrosine kinase signaling pathway contributes to neuroinflammation after subarachnoid hemorrhage in rats. Stroke 46(8):2277–2286. https://doi.org/10.1161/STROKEAHA.115.010088
26. de Rivero Vaccari JC, Brand FJ 3rd, Berti AF, Alonso OF, Bullock MR, de Rivero Vaccari JP (2015) Mincle signaling in the innate immune response after traumatic brain injury. J Neurotrauma 32(4):228–236. https://doi.org/10.1089/neu.2014.3436
27. Xie Y, Guo H, Wang L, Xu L, Zhang X, Yu L, Liu Q, Li Y et al (2017) Human albumin attenuates excessive innate immunity via inhibition of microglial Mincle/Syk signaling in subarachnoid hemorrhage. Brain Behav Immun 60:346–360. https://doi.org/10.1016/j.bbi.2016.11.004
28. Lee WB, Kang JS, Choi WY, Zhang Q, Kim CH, Choi UY, Kim-Ha J, Kim YJ (2016) Mincle-mediated translational regulation is required for strong nitric oxide production and inflammation resolution. Nat Commun 7:11322. https://doi.org/10.1038/ncomms11322
29. Xu Y, Xu Y, Wang Y, Wang Y, He L, Jiang Z, Huang Z, Liao H et al (2015) Telmisartan prevention of LPS-induced microglia activation involves M2 microglia polarization via CaMKKβ-dependent AMPK activation. Brain Behav Immun 50:298–313. https://doi.org/10.1016/j.bbi.2015.07.015
30. Lee CJ, Lee SS, Chen SC, Ho FM, Lin WW (2005) Oregonin inhibits lipopolysaccharide-induced iNOS gene transcription and upregulates HO-1 expression in macrophages and microglia. Br J Pharmacol 146(3):378–388. https://doi.org/10.1038/sj.bjp.0706336
31. Saura J, Tusell JM, Serratosa J (2003) High-yield isolation of murine microglia by mild trypsinization. Glia 44(3):183–189. https://doi.org/10.1002/glia.10274
32. Jo M, Kim JH, Song GJ, Seo M, Hwang EM, Suk K (2017) Astrocytic orosomucoid-2 modulates microglial activation and neuroinflammation. J Neurosci 37(11):2878–2894. https://doi.org/10.1523/JNEUROSCI.2534-16.2017
33. Lin YC, Huang DY, Chu CL, Lin YL, Lin WW (2013) The tyrosine kinase Syk differentially regulates Toll-like receptor signaling downstream of the adaptor molecules TRAF6 and TRAF3. Sci Signal 6(289):ra71. https://doi.org/10.1126/scisignal.2003973
34. Lin YC, Huang DY, Wang JS, Lin YL, Hsieh SL, Huang KC, Lin WW (2015) Syk is involved in NLRP3 inflammasome-mediated caspase-1 activation through adaptor ASC phosphorylation and enhanced oligomerization. J Leukoc Biol. doi:https://doi.org/10.1189/jlb.3HI0814-371RR

35. Orihuela R, McPherson CA, Harry GJ (2016) Microglial M1/M2 polarization and metabolic states. Br J Pharmacol 173(4):649–665. https://doi.org/10.1111/bph.13139
36. Sekar P, Huang DY, Chang SF, Lin WW (2018) Coordinate effects of P2X7 and extracellular acidification in microglial cells. Oncotarget 9 (16):12718–12731. doi:https://doi.org/10.18632/oncotarget.24331, 12718, 12731
37. Agger EM, Rosenkrands I, Hansen J, Brahimi K, Vandahl BS, Aagaard C, Werninghaus K, Kirschning C et al (2008) Cationic liposomes formulated with synthetic mycobacterial cordfactor (CAF01): a versatile adjuvant for vaccines with different immunological requirements. PLoS One 3(9):e3116. https://doi.org/10.1371/journal.pone.0003116
38. Milicic A, Kaur R, Reyes-Sandoval A, Tang CK, Honeycutt J, Perrie Y, Hill AV (2012) Small cationic DDA:TDB liposomes as protein vaccine adjuvants obviate the need for TLR agonists in inducing cellular and humoral responses. PLoS One 7(3):e34255. https://doi.org/10.1371/journal.pone.0034255
39. Henry CJ, Huang Y, Wynne A, Hanke M, Himler J, Bailey MT, Sheridan JF, Godbout JP (2008) Minocycline attenuates lipopolysaccharide (LPS)-induced neuroinflammation, sickness behavior, and anhedonia. J Neuroinflammation 5:15. https://doi.org/10.1186/1742-2094-5-15
40. Zanoni I, Ostuni R, Marek LR, Barresi S, Barbalat R, Barton GM, Granucci F, Kagan JC (2011) CD14 controls the LPS-induced endocytosis of Toll-like receptor 4. Cell 147(4):868–880. https://doi.org/10.1016/j.cell.2011.09.051
41. Lu R, Pan H, Shively JE (2012) CEACAM1 negatively regulates IL-1β production in LPS activated neutrophils by recruiting SHP-1 to a SYK-TLR4-CEACAM1 complex. PLoS Pathog 8(4): e1002597. https://doi.org/10.1371/journal.ppat.1002597
42. Honjoh C, Chihara K, Yoshiki H, Yamauchi S, Takeuchi K, Kato Y, Hida Y, Ishizuka T et al (2017) Association of C-type lectin Mincle with FcεRIβγ subunits leads to functional activation of RBL-2H3 cells through Syk. Sci Rep 7:46064. https://doi.org/10.1038/srep46064
43. Grahame Hardie D (2014) AMP-activated protein kinase: a key regulator of energy balance with many roles in human disease. J Intern Med 276(6):543–559. https://doi.org/10.1111/joim.12268
44. Racioppi L, Noeldner PK, Lin F, Arvai S, Means AR (2012) Calcium/calmodulin-dependent protein kinase kinase 2 regulates macrophage-mediated inflammatory responses. J Biol Chem 287(14):11579–11591. https://doi.org/10.1074/jbc.M111.336032
45. Du L, Zhang Y, Chen Y, Zhu J, Yang Y, Zhang HL (2016) Role of microglia in neurological disorders and their potentials as a therapeutic target. Mol Neurobiol 54:7567–7584. https://doi.org/10.1007/s12035-016-0245-0
46. Schoenen H, Huber A, Sonda N, Zimmermann S, Jantsch J, Lepenies B, Bronte V, Lang R (2014) Differential control of Mincle-dependent cord factor recognition and macrophage responses by the transcription factors C/EBPβ and HIF1α. J Immunol 193(7):3664–3675. https://doi.org/10.4049/jimmunol.1301593
47. Block ML, Zecca L, Hong JS (2007) Microglia-mediated neurotoxicity: uncovering the molecular mechanisms. Nat Rev Neurosci 8(1):57–69. https://doi.org/10.1038/nrn2038
48. Greco SH, Mahmood SK, Vahle AK, Ochi A, Batel J, Deutsch M, Barilla R, Seifert L et al (2016) Mincle suppresses Toll-like receptor 4 activation. J Leukoc Biol 100(1):185–194. https://doi.org/10.1189/jlb.3A0515-185R
49. Arumugam TV, Manzanero S, Furtado M, Biggins PJ, Hsieh YH, Gelderblom M, MacDonald KP, Salimova E et al (2017) An atypical role for the myeloid receptor Mincle in central nervous system injury. J Cereb Blood Flow Metab 37(6):2098–2111. https://doi.org/10.1177/0271678X16661201
50. Lv LL, Tang PM, Li CJ, You YK, Li J, Huang XR, Ni J, Feng M et al (2017) The pattern recognition receptor, Mincle, is essential for maintaining the M1 macrophage phenotype in acute renal inflammation. Kidney Int 91(3):587–602. https://doi.org/10.1016/j.kint.2016.10.020
51. Zhao XQ, Zhu LL, Chang Q, Jiang C, You Y, Luo T, Jia XM, Lin X (2014) C-type lectin receptor dectin-3 mediates trehalose 6,6′-dimycolate (TDM)-induced Mincle expression through CARD9/Bcl10/MALT1-dependent nuclear factor (NF)-κB activation. J Biol Chem 289(43):30052–30062. https://doi.org/10.1074/jbc.M114.588574
52. Dambuza IM, Brown GD (2015) C-type lectins in immunity: recent developments. Curr Opin Immunol 32:21–27. https://doi.org/10.1016/j.coi.2014.12.002
53. Mocsai A, Ruland J, Tybulewicz VL (2010) The SYK tyrosine kinase: a crucial player in diverse biological functions. Nat Rev Immunol 10(6):387–402. https://doi.org/10.1038/nri2765
54. Zong Y, Ai QL, Zhong LM, Dai JN, Yang P, He Y, Sun J, Ling EA et al (2012) Ginsenoside Rg1 attenuates lipopolysaccharide-induced inflammatory responses via the phospholipase C-gamma1 signaling pathway in murine BV-2 microglial cells. Curr Med Chem 19(5):770–779
55. Yang WS, Jeong D, Yi YS, Lee BH, Kim TW, Htwe KM, Kim YD, Yoon KD et al (2014) Myrsine seguinii ethanolic extract and its active component quercetin inhibit macrophage activation and peritonitis induced by LPS by targeting to Syk/Src/IRAK-1. J Ethnopharmacol 151(3):1165–1174. https://doi.org/10.1016/j.jep.2013.12.033
56. Yin H, Zhou H, Kang Y, Zhang X, Duan X, Alnabhan R, Liang S, Scott DA et al (2016) Syk negatively regulates TLR4-mediated IFNβ and IL-10 production and promotes inflammatory responses in dendritic cells. Biochim Biophys Acta 1860(3):588–598. https://doi.org/10.1016/j.bbagen.2015.12.012
57. Han C, Jin J, Xu S, Liu H, Li N, Cao X (2010) Integrin CD11b negatively regulates TLR-triggered inflammatory responses by activating Syk and promoting degradation of MyD88 and TRIF via Cbl-b. Nat Immunol 11(8):734–742. https://doi.org/10.1038/ni.1908
58. Hou CH, Lin J, Huang SC, Hou SM, Tang CH (2009) Ultrasound stimulates NF-kappaB activation and iNOS expression via the Ras/Raf/MEK/ERK signaling pathway in cultured preosteoblasts. J Cell Physiol 220(1):196–203. https://doi.org/10.1002/jcp.21751
59. Lin CC, Shih CH, Yang YL, Bien MY, Lin CH, Yu MC, Sureshbabu M, Chen BC (2011) Thrombin induces inducible nitric oxide synthase expression via the MAPK, MSK1, and NF-κB signaling pathways in alveolar macrophages. Eur J Pharmacol 672(1–3):180–187. https://doi.org/10.1016/j.ejphar.2011.10.005
60. Carter AB, Hunninghake GW (2000) A constitutive active MEK → ERK pathway negatively regulates NF-κB-dependent gene expression by modulating TATA-binding protein phosphorylation. J Biol Chem 275(36):27858–27864. https://doi.org/10.1074/jbc.M003599200
61. Maeng YS, Min JK, Kim JH, Yamagishi A, Mochizuki N, Kwon JY, Park YW, Kim YM et al (2006) ERK is an anti-inflammatory signal that suppresses expression of NF-κB-dependent inflammatory genes by inhibiting IKK activity in endothelial cells. Cell Signal 18(7):994–1005. https://doi.org/10.1016/j.cellsig.2005.08.007
62. Ahmed KM, Dong S, Fan M, Li JJ (2006) Nuclear factor-kappaB p65 inhibits mitogen-activated protein kinase signaling pathway in radioresistant breast cancer cells. Mol Cancer Res 4(12):945–955. https://doi.org/10.1158/1541-7786.MCR-06-0291
63. Oyesanya RA, Lee ZP, Wu J, Chen J, Song Y, Mukherjee A, Dent P, Kordula T et al (2008) Transcriptional and post-transcriptional mechanisms for lysophosphatidic acid-induced cyclooxygenase-2 expression in ovarian cancer cells. FASEB J 22(8):2639–2651. https://doi.org/10.1096/fj.07-101428

64. Kang YJ, Mbonye UR, DeLong CJ, Wada M, Smith WL (2007) Regulation of intracellular cyclooxygenase levels by gene transcription and protein degradation. Prog Lipid Res 46(2):108–125. https://doi.org/10.1016/j.plipres.2007.01.001
65. Hardie DG, Ross FA, Hawley SA (2012) AMPK: a nutrient and energy sensor that maintains energy homeostasis. Nat Rev Mol Cell Biol 13(4):251–262. https://doi.org/10.1038/nrm3311
66. Amato S, Man HY (2011) Bioenergy sensing in the brain: the role of AMP-activated protein kinase in neuronal metabolism, development and neurological diseases. Cell Cycle 10(20):3452–3460. https://doi.org/10.4161/cc.10.20.17953
67. Li J, McCullough LD (2010) Effects of AMP-activated protein kinase in cerebral ischemia. J Cereb Blood Flow Metab 30(3): 480–492. https://doi.org/10.1038/jcbfm.2009.255
68. Giri S, Nath N, Smith B, Viollet B, Singh AK, Singh I (2004) 5-aminoimidazole-4-carboxamide-1-beta-4-ribofuranoside inhibits proinflammatory response in glial cells: a possible role of AMP-activated protein kinase. J Neurosci 24(2):479–487. https://doi.org/10.1523/JNEUROSCI.4288-03.2004
69. Nath N, Khan M, Paintlia MK, Singh I, Hoda MN, Giri S (2009) Metformin attenuated the autoimmune disease of the central nervous system in animal models of multiple sclerosis. J Immunol 182(12):8005–8014. https://doi.org/10.4049/jimmunol.0803563
70. Mounier R, Theret M, Arnold L, Cuvellier S, Bultot L, Goransson O, Sanz N, Ferry A et al (2013) AMPKα1 regulates macrophage skewing at the time of resolution of inflammation during skeletal muscle regeneration. Cell Metab 18(2):251–264. https://doi.org/10.1016/j.cmet.2013.06.017